FOXO1 differentially regulates both normal and diabetic wound healing

Chenying Zhang,[1,2] Bhaskar Ponugoti,[2] Chen Tian,[2] Fanxing Xu,[2,3] Rohinton Tarapore,[2] Angelika Batres,[2] Sarah Alsadun,[2] Jason Lim,[2] Guangyu Dong,[2] and Dana T. Graves[2]

[1]Department of Preventive Dentistry, Peking University School and Hospital of Stomatology, Beijing 100081, China
[2]Department of Periodontics, School of Dental Medicine, University of Pennsylvania, Philadelphia, PA 19104
[3]School of Life Science and Biotechnology, Dalian University of Technology, Dalian 116024, China

Healing is delayed in diabetic wounds. We previously demonstrated that lineage-specific *Foxo1* deletion in keratinocytes interfered with normal wound healing and keratinocyte migration. Surprisingly, the same deletion of *Foxo1* in diabetic wounds had the opposite effect, significantly improving the healing response. In normal glucose media, forkhead box O1 (FOXO1) enhanced keratinocyte migration through up-regulating TGFβ1. In high glucose, FOXO1 nuclear localization was induced but FOXO1 did not bind to the *TGFβ1* promoter or stimulate *TGFβ1* transcription. Instead, in high glucose, FOXO1 enhanced expression of serpin peptidase inhibitor, clade B (ovalbumin), member 2 (SERPINB2), and chemokine (C-C motif) ligand 20 (CCL20). The impact of high glucose on keratinocyte migration was rescued by silencing FOXO1, by reducing SERPINB2 or CCL20, or by insulin treatment. In addition, an advanced glycation end product and tumor necrosis factor had a similar regulatory effect on FOXO1 and its downstream targets and inhibited keratinocyte migration in a FOXO1-dependent manner. Thus, FOXO1 expression can positively or negatively modulate keratinocyte migration and wound healing by its differential effect on downstream targets modulated by factors present in diabetic healing.

Introduction

Wound healing involves a complex series of events characterized by inflammation, migration, proliferation, and remodeling (Reinke and Sorg, 2012). Diabetes impairs wound healing, which leads to considerable morbidity and may result in limb amputation (Moulik et al., 2003). The underlying mechanisms of defective wound repair in diabetic patients are not completely understood (Gary Sibbald and Woo, 2008; Xu et al., 2013). Enhanced levels of advanced glycation end products (AGEs) and TNF are associated with altered diabetic wound healing. Impaired wound healing responses in diabetic animals are improved by blocking TNF, or AGEs, which reduces infiltration by proinflammatory macrophages, reduces fibroblast apoptosis, and improves collagen deposition (Goova et al., 2001; Goren et al., 2007; Siqueira et al., 2010; Ashcroft et al., 2012). Moreover, reducing inflammation by deletion of TLR4 improves the wound healing response (Dasu and Jialal, 2013).

Reepithelialization is an essential step in the wound healing process and is driven by migration and proliferation of keratinocytes (Coulombe, 2003). Migration appears to be the most important cellular activity for reepithelialization because defects in migration are closely associated with poorly healing wounds (Andriessen et al., 1995; Stojadinovic et al., 2005). In normal wound healing, keratinocyte migration is regulated by growth factors, integrins, extracellular matrix molecules, and metalloproteinases (Raja et al., 2007). Although there have been numerous studies on wound healing in diabetes, relatively little is known regarding the molecular deficits in diabetic impaired reepithelialization.

Forkhead box O1 (FOXO1) belongs to a large family of forkhead transcription factors characterized by a conserved DNA binding domain. FOXO1 modulates expression of genes involved in apoptosis, cell cycle progression, DNA repair, oxidative stress resistance, cell differentiation, and glucose metabolism (Huang and Tindall, 2007). Because of their importance

The Rockefeller University Press $30.00
J. Cell Biol. Vol. 209 No. 2 289–303
www.jcb.org/cgi/doi/10.1083/jcb.201409032

JCB **289**

THE JOURNAL OF CELL BIOLOGY

in maintaining cellular homeostasis, FOXO1 is tightly regulated by a sophisticated signaling network that includes inactivation by insulin and growth factors that exclude FOXO1 from the nucleus (Barthel et al., 2005). It is striking that the impact of FOXO1 is often evident under stressed conditions such as diabetes as a result of the responsiveness of FOXO1 to environmental changes (Eijkelenboom and Burgering, 2013). Factors that are increased by diabetes, such as TNF and AGEs, stimulate FOXO1 activation (Alikhani et al., 2007; Behl et al., 2009; Ponugoti et al., 2012). FOXO1 is up-regulated by wound healing, particularly in diabetic animals (Siqueira et al., 2010). Moreover, *Foxo1* deletion in keratinocytes impairs the healing response, indicating that FOXO1 promotes reepithelialization in normoglycemic conditions (Ponugoti et al., 2013). One of the primary mechanisms through which FOXO1 was shown to enhance healing was up-regulation of TGFβ1. Because its functional role in diabetic healing has not been investigated we performed experiments to address this issue. Surprisingly, lineage-specific deletion of *Foxo1* led to enhanced wound healing behavior of keratinocytes. Thus, in diabetic mice, FOXO1 has the opposite effect on keratinocyte wound healing behavior as it does under normal conditions. The differential effect of FOXO1 on normal and diabetic healing was caused by changes in its regulation of downstream targets, which was modulated by factors that are elevated in diabetes. In normal conditions, FOXO1 binds to the *TGFβ1* promoter and up-regulates TGFβ1 expression, which is crucial for keratinocyte migration. When stimulated with high glucose, AGEs, or TNF, FOXO1 fails to bind to the *TGFβ1* promoter and does not up-regulate TGFβ1 expression. Instead, FOXO1 enhances the expression of factors that lead to reduced keratinocyte migration. Moreover, insulin rescued the negative effect of these factors on keratinocyte through migration through Akt, which blocks FOXO1. This provides a mechanistic explanation for impaired reepithelialization in situations where the levels of glucose, AGEs, and TNF are elevated, such as diabetes.

Results

Keratinocyte-specific *Foxo1* deletion delays wound healing in normoglycemic mice while improving wound repair in diabetic mice

Small excisional skin wounds were created in experimental transgenic mice (K14.Cre$^+$.*Foxo1$^{L/L}$*) with keratinocyte-specific deletion of *Foxo1* driven by keratin-14 Cre recombinase and littermate control (K14.Cre$^-$.*Foxo1$^{L/L}$*) mice without *Foxo1* deletion. Deletion of *Foxo1* in keratinocytes of nondiabetic mice delayed wound healing (Fig. 1 A and Fig. S1 A). In contrast, lineage-specific deletion of *Foxo1* in diabetic mice had the opposite effect, accelerating wound closure. Normoglycemic mice with *Foxo1* deletion had up to twofold larger wounds compared with matched littermate controls (P < 0.05; Fig. 1 A). In contrast, wounds in diabetic experimental *Foxo1*-deficient mice were reduced by 30–60% compared with diabetic control mice (Fig. 1 A). At the histological level, keratinocyte-specific *Foxo1* deletion in normoglycemic mice resulted in up to twofold larger wounds, whereas *Foxo1* deletion in diabetic mice reduced

wound size by 40–80% compared with matched control littermates (P < 0.05; Fig. S1 A and Table 1). Lineage-specific deletion of *Foxo1* in diabetic mice improved healing by increasing epithelial thickness and epithelial area of healing wounds so they reached levels similar to normal mice (P < 0.05; Table 1). In contrast, *Foxo1* deletion in normoglycemic mice had the opposite effect on the epithelial area and thickness in healing wounds (Table 1).

Because it was possible that differential expression of FOXO1 was responsible for the variable effect of *Foxo1* deletion on normal and diabetic wound healing, FOXO1 nuclear translocation and expression was assessed. Diabetic control mice had higher levels of FOXO1 nuclear localization compared with normoglycemic control mice (Fig. 1 B and Fig. S1 B). The overall level of FOXO1 expression at the protein level and the mRNA level was increased in wounded compared with nonwounded epithelium in both normal and diabetic mice (Fig. S1, C and D). As expected, FOXO1 nuclear localization and expression were significantly reduced by 80–90% in keratinocytes of experimental versus control mice (Fig. 1 B; and Fig. S1, C and D). Thus, the different effect of FOXO1 on wound healing behavior in normal and diabetic mice was not caused by a failure to induce FOXO1 in keratinocytes of diabetic animals. This was also demonstrated in vitro as high glucose significantly increased FOXO1 nuclear localization in a time-dependent manner in primary cultures of murine keratinocytes isolated from K14.Cre$^-$.*Foxo1$^{L/L}$* mice (P < 0.05; Fig. 1 C). In addition, high glucose also apparently increased FOXO1 DNA binding in primary cultures of normal human epidermal keratinocytes (NHEKs) compared with low glucose (P < 0.05; Fig. 1 D).

FOXO1 silencing reduces the closure of in vitro scratch wounds in low glucose conditions, whereas it improves in vitro wound closure in high glucose conditions

To determine whether the effect of FOXO1 on wound healing was directly related to glucose levels, an in vitro scratch assay was performed under defined conditions and reepithelialization of the denuded area was measured (Fig. S2). Transfection of NHEK cells with FOXO1 siRNA significantly reduced FOXO1 mRNA levels by 80–90% compared with scrambled siRNA (P < 0.05; Fig. S1 E) and significantly reduced FOXO1 DNA binding activity (Fig. 1 D). Under low glucose conditions, knockdown of FOXO1 significantly reduced the reepithelialization of the in vitro scratch wound by 35–50% (P < 0.05), whereas knockdown of FOXO3 had no effect compared with scrambled control siRNA (P > 0.05; Fig. 1 E). In contrast, under high glucose conditions, FOXO1 knockdown significantly increased reepithelialization in vitro by 55–70% (P < 0.05), whereas FOXO3 knockdown had no effect (P > 0.05; Fig. 1 F). Thus, in vitro experiments in high glucose mimicked the effect of diabetes, and the positive impact of FOXO1 deletion on both was consistent. In contrast, overexpression of constitutively active FOXO1 (FOXO1-AAA) significantly increased reepithelialization of the scratch wound in low glucose but in high glucose FOXO1 overexpression had the opposite effect, reducing reepithelialization (P < 0.05; Fig. 1, G and H).
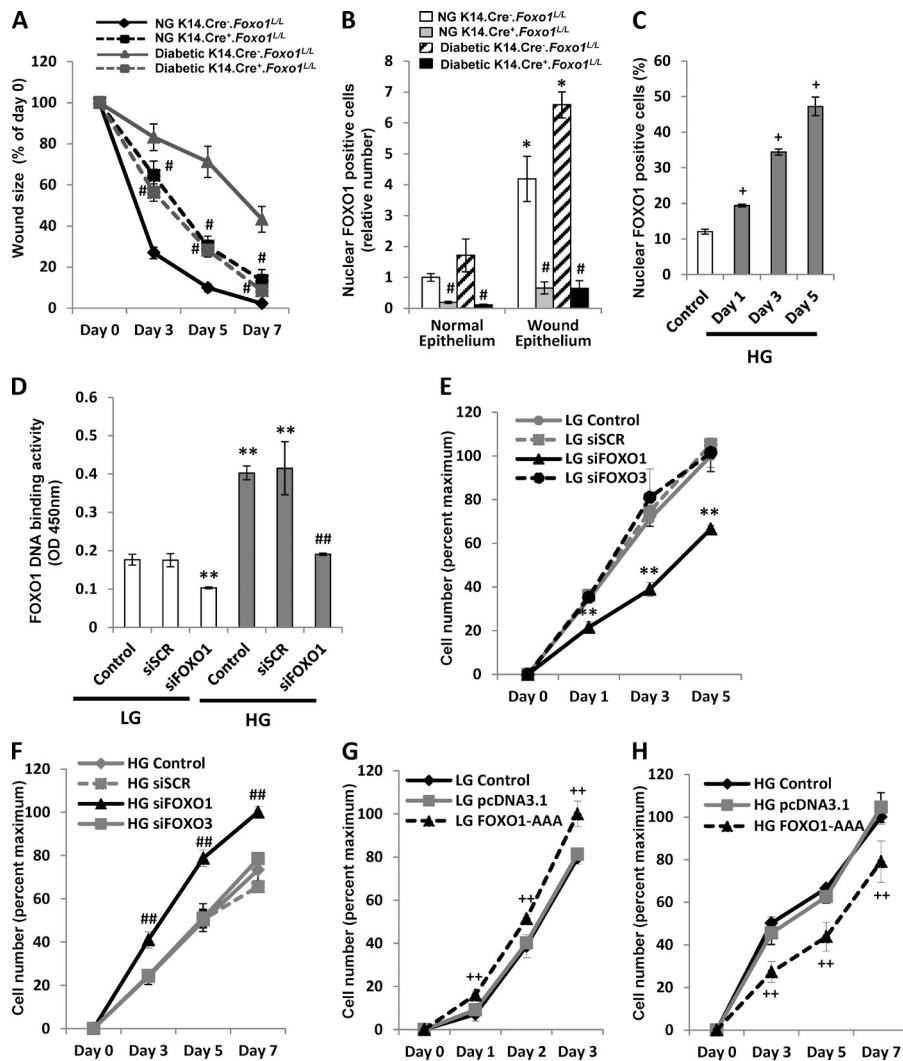
Figure 1. **Keratinocyte-specific *Foxo1* deletion impairs normoglycemic wound healing but enhances diabetic wound healing.** (A) The percentage of wound closure was measured in normoglycemic (NG) and diabetic control K14.Cre⁻.*Foxo1*^L/L and experimental K14.Cre⁺.*Foxo1*^L/L mice. Wound size was compared with day 0. (B) FOXO1 nuclear localization was determined by colocalization of FOXO1 determined by immunofluorescence and nuclear staining by DAPI for day 4 wounds. Data are presented as the ratio of keratinocytes with nuclear FOXO1 compared with nuclear FOXO1 in normal control epithelium. (C) Quantification of FOXO1 nuclear localization in NHEK cells incubated in high glucose (HG) media. (D–H) NHEK cells were transfected with scrambled siRNA (siSCR) or siRNA specific for FOXO1 or FOXO3 (D–F), or transfected with control plasmid or constitutively active FOXO1 plasmid (G and H) in low (LG) and high glucose media. (D) FOXO1 DNA binding activity of nuclear proteins was measured by transcription factor ELISA. (E–H) Quantitative analyses of keratinocytes closing a scratch wound incubated in low (E and G) or high (F and H) glucose culture media. Each in vivo value represents the mean ± SEM; $n = 5$–8 per group. Each in vitro data represent the mean ± SEM of three independent experiments. #, $P < 0.05$ versus matched Cre⁻ group; *, $P < 0.05$ versus normal epithelium; ⁺, $P < 0.05$ versus low glucose control; **, $P < 0.05$ versus low glucose scrambled siRNA; ##, $P < 0.05$ versus high glucose scrambled siRNA; ⁺⁺, $P < 0.05$ versus control plasmid.

FOXO1 deficiency reduces migration in low glucose conditions, whereas it has the opposite effect in high glucose conditions

To investigate mechanisms through which FOXO1 affected wound healing, keratinocyte migration and proliferation were assessed in vivo. Wounding increased keratinocyte migration as determined by expression of urokinase-type plasminogen activator receptor (uPAR; Fig. 2 A), a marker of keratinocyte migration (Lund et al., 2006). Diabetes had a significant negative effect on migration of keratinocytes ($P < 0.05$; Fig. 2 A and Fig. S3 A). *Foxo1* ablation in diabetic mice increased migration twofold compared with diabetic control littermates ($P < 0.05$). The effect of *Foxo1* deletion increased keratinocyte migration to a level that was similar to normoglycemic mice (Fig. 2 A). In

Table 1. **Histological change of the mice scalp wound**

Wound parameter	Day	Normoglycemic			Diabetic		
		K14.Cre⁻.*Foxo1*^L/L	K14.Cre⁺.*Foxo1*^L/L	Cre⁺/Cre⁻	K14.Cre⁻.*Foxo1*^L/L	K14.Cre⁺.*Foxo1*^L/L	Cre⁺/Cre⁻
Epithelial gap (mm)	4	0.59 ± 0.27	1.76 ± 0.08ᵃ	2.98	1.66 ± 0.08	1.01 ± 0.17ᵇ	0.61
	7	0.35 ± 0.28	0.56 ± 0.36ᵃ	1.60	1.52 ± 0.13	0.29 ± 0.18ᵇ	0.19
Epithelial thickness (mm)	4	0.09 ± 0.01	0.06 ± 0.01ᵃ	0.67	0.07 ± 0.01	0.10 ± 0.01ᵇ	1.43
	7	0.08 ± 0.01	0.05 ± 0.01ᵃ	0.63	0.06 ± 0.01	0.08 ± 0.01ᵇ	1.33
Epithelial area (mm²)	4	0.21 ± 0.02	0.11 ± 0.02ᵃ	0.52	0.17 ± 0.01	0.23 ± 0.02ᵇ	1.35
	7	0.18 ± 0.01	0.10 ± 0.02ᵃ	0.56	0.10 ± 0.01	0.16 ± 0.01ᵇ	1.60

All numbers are means ± SEM.
[a]Significant change compared to normoglycemic K14.Cre⁻.*Foxo1*^L/L mice ($P < 0.05$).
[b]Significant change compared to diabetic K14.Cre⁻.*Foxo1*^L/L mice ($P < 0.05$).

Figure 2. **Foxo1 deletion enhances keratinocyte migration and proliferation in diabetic specimens or in keratinocytes incubated in high glucose in vitro.** uPAR (A) and PCNA (B) immunofluorescence analyses for day 4 wounds from normoglycemic (NG) and diabetic K14.Cre⁻.Foxo1^{L/L} and K14.Cre⁺.Foxo1^{L/L} mice. Data are presented as a ratio of the number of uPAR or PCNA immunopositive keratinocytes divided by the number of immunopositive keratinocytes in nonwounded epithelium of control mice. (C and D) Migration was measured in a transwell assay for NHEK cells transfected with scrambled or FOXO1 siRNA in low and high glucose media (C) or under the stimulation of indicated doses of D-glucose (D). (E–J) Primary murine keratinocytes from K14.Cre⁻.Foxo1^{L/l} or K14.Cre⁺.Foxo1^{L/L} mice were incubated in low and high glucose media. (E–G) FOXO1 immunofluorescence analyses were performed to measure FOXO1 mean fluorescence intensity (E), percentage of FOXO1 immunopositive cells (F), and FOXO1 nuclear localization (G). (H) Western blot for cytoplasmic and nuclear FOXO1 expression in K14.Cre⁻.Foxo1^{L/L} keratinocytes. (I) Migration was assessed by transwell migration assay. (J) DNA synthesis of primary murine keratinocytes was determined by BrdU incorporation ELISA. Each in vitro experiment represents the mean ± SEM of three independent experiments; n = 5–8 per group for in vivo experiments. *, P < 0.05 versus Cre⁻ group; **, P < 0.05 versus normal epithelium; #, P < 0.05 versus matched normoglycemic or low glucose control group; +, P < 0.05 versus scrambled siRNA.
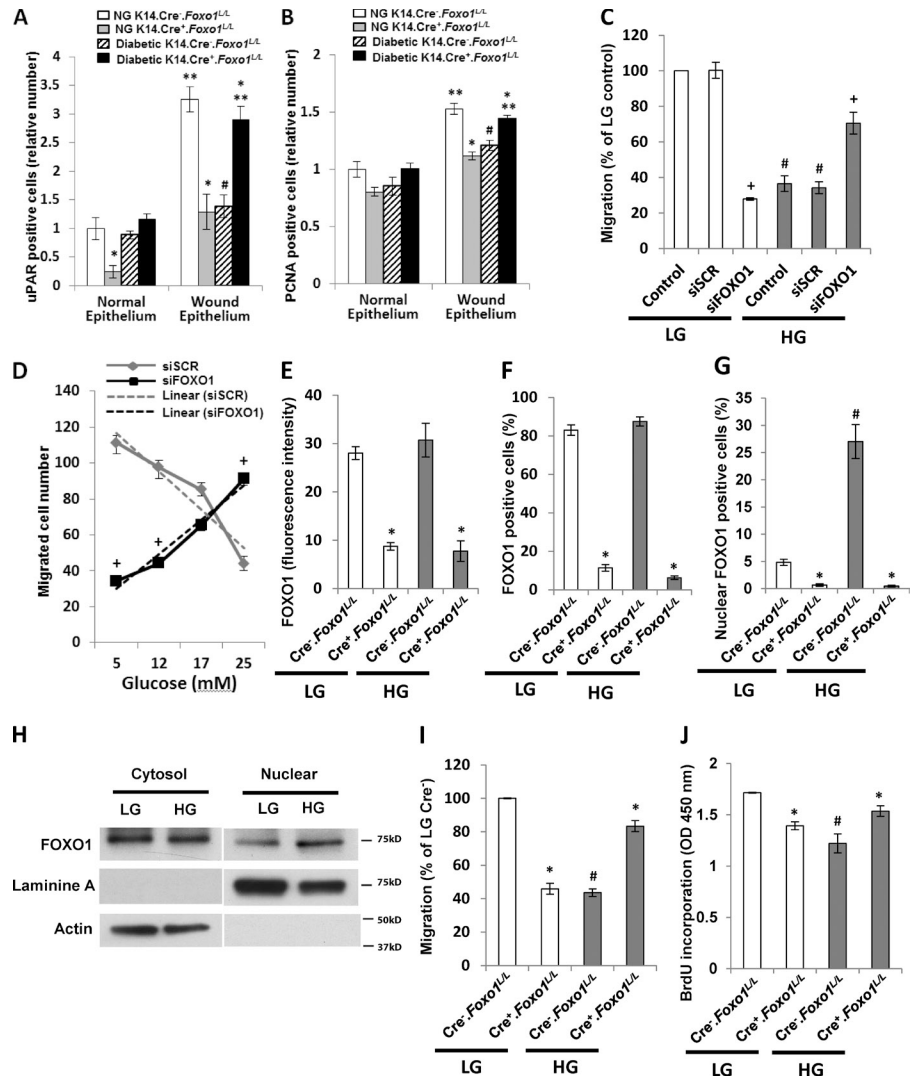
contrast, *Foxo1* ablation in normoglycemic mice decreased the number of migrating keratinocytes by 60% compared with matched controls (P < 0.05; Fig. 2 A).

Foxo1 deletion in normoglycemic mice caused a small but significant 27% reduction in the number of proliferating cell nuclear antigen (PCNA)–positive proliferating keratinocytes in wound epithelium (P < 0.05; Fig. 2 B). In contrast, *Foxo1* deletion in diabetic mice increased PCNA-positive keratinocytes by 20% (P < 0.05; Fig. 2 B). Notably, the magnitude of the positive effect of *Foxo1* deletion in vivo on keratinocyte proliferation in diabetic mice was not as great as the effect on migration: 1.2-fold versus twofold.

The effect of FOXO1 on keratinocyte migration was investigated further in vitro in a transwell migration assay. Similar to in vivo results, keratinocyte migration in high glucose in vitro was reduced 64% compared with standard media (P < 0.05; Fig. 2 C). Migration was not affected by mannitol, a high glucose osmotic control (Fig. S3 B). Knockdown of FOXO1 reduced keratinocyte migration by ~70% in low glucose media (P < 0.05) but increased keratinocyte migration more than twofold in high glucose compared with matched scrambled control (P < 0.05;

Fig. 2 C). In contrast, knockdown of FOXO1 had little effect on keratinocyte proliferation both in low glucose and high glucose (Fig. S3 C). The effect of different glucose concentrations in modulating keratinocyte migration in a FOXO1-dependent manner was tested (Fig. 2 D). Glucose reduced keratinocyte migration in control cells but had the opposite effect when FOXO1 was deleted. The tipping point where FOXO1 deletion had no effect was ~19 mM glucose.

These studies examined the effect of FOXO1 knockdown in primary cultures of human keratinocytes. The differential impact of FOXO1 was also examined in primary cultures of murine keratinocytes isolated from K14.Cre⁻.Foxo1^{L/L} and K14.Cre⁺.Foxo1^{L/L} mice. FOXO1 protein levels were not increased by high glucose (Fig. 2, E and F) but FOXO1 nuclear localization was increased 5.6-fold in keratinocytes from K14.Cre⁻.Foxo1^{L/L} control mice in high glucose condition (P < 0.05; Fig. 2 G). Moreover, FOXO1 expression was reduced by 70–90% and FOXO1 nuclear localization by >90% in keratinocytes from experimental mice compared with keratinocytes from control mice (P < 0.05; Fig. 2, E–G). In agreement with immunofluorescent studies, Western blot analysis also showed that high glucose
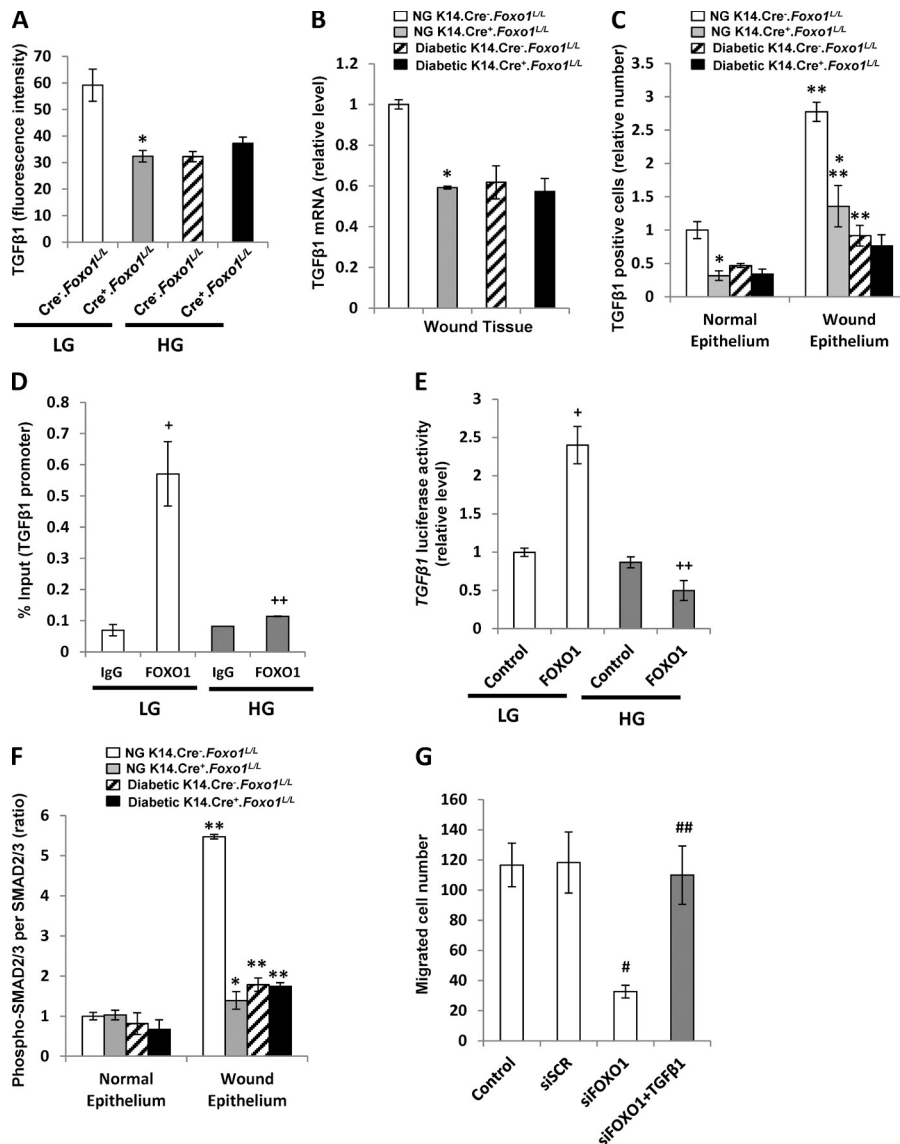
Figure 3. **FOXO1 modulates normoglycemic wound healing by regulating TGFβ1 but does not regulate TGFβ1 in diabetic healing.** Primary murine keratinocytes (A) or wound tissue (B, C, and F) were collected from K14.Cre⁻.Foxo1^{L/L} and K14.Cre⁺.Foxo1^{L/L} mice. (A) TGFβ1 immunofluorescence analyses for murine keratinocytes. (B) TGFβ1 mRNA levels were assessed by quantitative RT-PCR for day 4 wounds. (C) TGFβ1 immunofluorescence analyses for day 4 wounds. (D) ChIP assays for the binding of FOXO1 to the TGFβ1 promoter in NHEK cells. ChIP-enriched DNA was quantified by quantitative RT-PCR and values were expressed as a percentage of input DNA. (E) TGFβ1 luciferase reporter gene analyses in NHEK cells after cotransfection with control or FOXO1 plasmid. (F) phospho-SMAD2/3 immunofluorescence analyses for day 4 wounds. (G) Keratinocyte migration was assessed in a transwell assay for NHEK cells transfected with scrambled or FOXO1 siRNA with or without TGFβ1 in low glucose media. Each in vivo value is the mean ± SEM for n = 5–8 mice per group. In vitro values represent the mean ± SEM of three independent experiments. *, P < 0.05 versus Cre⁻ group; **, P < 0.05 versus normal epithelium; ⁺, P < 0.05 versus matched control plasmid or IgG control; ⁺⁺, P < 0.05 versus low glucose group; #, P < 0.05 versus scrambled siRNA; ##, P < 0.05 versus siFOXO1 group.

increased FOXO1 nuclear localization in keratinocytes from control mice, whereas it had little effect on overall FOXO1 expression levels (Fig. 2 H), consistent with results from diabetic mice in vivo.

The effect of glucose on migration of primary murine keratinocytes isolated from normal and experimental mice was also examined. In high glucose media, *Foxo1* ablation increased keratinocyte migration twofold (P < 0.05; Fig. 2 I). In contrast, deletion of *Foxo1* reduced murine keratinocyte migration by 54% when cells were incubated in standard glucose media (P < 0.05; Fig. 2 I). Results examining migration of murine keratinocytes from mice with *Foxo1* deleted by Cre recombinase agreed well with experiments with human NHEK cells that had FOXO1 knockdown by siRNA. Similarly, *Foxo1* deletion in murine keratinocytes largely reversed the small but significant negative effect of high glucose on murine keratinocyte proliferation (P < 0.05; Fig. 2 J). Thus, the large glucose-dependent effect of *Foxo1* deletion on murine keratinocyte migration and small effect on proliferation was similar to that observed

for human keratinocytes and consistent with results obtained in vivo with diabetic mice. Collectively, these results point to the dramatic positive effect of *Foxo1* deletion under high glucose conditions and, combined with in vivo data, suggest that the effect on keratinocyte migration represents an important mechanism by which FOXO1 affects reepithelialization and wound healing.

FOXO1 regulation of TGFβ1 is dependent on glucose levels in vitro and diabetic condition in vivo

Foxo1 deletion in vitro reduced TGFβ1 levels by 45% in standard glucose media (P < 0.05; Fig. 3 A). High glucose in vitro also reduced TGFβ1 expression. However, *Foxo1* deletion in high glucose had no effect on TGFβ1 expressionm, indicating that in high glucose media FOXO1 does not regulate TGFβ1 (P > 0.05; Fig. 3 A). *Foxo1* deletion in vivo also significantly reduced TGFβ1 mRNA levels in wounds from normoglycemic mice but *Foxo1* deletion had little effect on its mRNA levels in

diabetic mice (P > 0.05; Fig. 3 B). The differential regulation of TGFβ1 by FOXO1 in normoglycemic and diabetic mice was further confirmed at the protein level. When *Foxo1* was deleted in normoglycemic mice the number of TGFβ1-positive keratinocytes was reduced by 50% compared with littermate controls (Fig. 3 C). However, *Foxo1* ablation in diabetic mice did not affect the number of keratinocytes that expressed TGFβ1 (P > 0.05; Fig. 3 C). This is consistent with the concept that FOXO1 plays a role in TGFβ1 expression under normal conditions but not in diabetic or high glucose conditions.

Chromatin immunoprecipitation (ChIP) assays showed that FOXO1 interacted with the *TGFβ1* promoter under low glucose conditions (Fig. 3 D). High glucose blocked FOXO1–*TGFβ1* promoter interactions (Fig. 3 D). We then determined whether glucose levels modulated the capacity of FOXO1 to transcriptionally regulate TGFβ1 using a TGFβ1 reporter. Overexpression of FOXO1 increased *TGFβ1* promoter activity in low glucose, but in high glucose FOXO1 overexpression had no effect on *TGFβ1* promoter activity (Fig. 3 E). Thus, glucose levels determine whether FOXO1 binds to the *TGFβ1* promoter and regulates *TGFβ1* transcriptional activity.

SMAD2/3 phosphorylation is downstream of TGFβ1 and represents a functional test of the degree of TGFβ1 signaling. Lineage-specific *Foxo1* ablation reduced SMAD2/3 phosphorylation by 75% in keratinocytes in wounds of normoglycemic mice in vivo (P < 0.05; Fig. 3 F). However, deletion of *Foxo1* in diabetic mice had no effect on phospho-SMAD2/3 levels compared with diabetic control mice (P > 0.05; Fig. 3 F). The lack of an effect of *Foxo1* ablation on this functional assay in diabetic mice is consistent with the failure of FOXO1 to regulate TGFβ1 under these conditions. In contrast, deletion of *Foxo1* in normoglycemic mice has a significant effect on TGFβ1 signaling.

One of the principal mechanisms by which TGFβ1 affects wound healing is regulation of keratinocyte migration (Gailit, et al., 1994). We determined functionally whether treatment with TGFβ1 could rescue deficits in keratinocyte migration. Notably, the reduced migration caused by FOXO1 knockdown was rescued by TGFβ1 (Fig. 3 G). This suggests that in low glucose conditions the TGFβ1 deficit caused by FOXO1 deletion is problematic.

FOXO1 regulation of SERPINB2 and CCL20 is dependent on glucose levels in vitro and presence of diabetes in vivo

Microarray analysis was performed to further investigate potential inhibitory factors regulated by FOXO1 (Table S1). Two of these, serpin peptidase inhibitor, clade B (ovalbumin), member 2 (SERPINB2), and chemokine (C-C motif) ligand 20 (CCL20) were chosen for further analysis because they have previously been shown to be involved in wound healing (Yamazaki et al., 2008; Tarcic et al., 2012). High glucose induced a 6.4-fold increase in SERPINB2 mRNA levels in NHEK cells in vitro (P < 0.05), and knockdown of FOXO1 reduced SERPINB2 mRNA levels by 94% (P < 0.05; Fig. 4 A). At the protein level, high glucose increased SERPINB2 expression three- to fourfold (P < 0.05), and this increase was blocked by *Foxo1* ablation

in keratinocytes (P < 0.05; Fig. 4, B and C). Whether or not FOXO1 regulated SERPINB2 in vivo was investigated in diabetic wounds (Fig. S4 A). Keratinocytes in diabetic wounds had a twofold increase in SERPINB2 compared with matched normoglycemic mice (P < 0.05; Fig. 4 D and Fig. S4 B). Deletion of *Foxo1* in vivo by Cre recombinase blocked diabetes-enhanced SERPINB2 expression (P < 0.05; Fig. 4 D and Fig. S4 B), demonstrating that the impact of diabetes on SERPINB2 is FOXO1 dependent. ChIP assays were then conducted and determined that FOXO1 interacted with the *SERPINB2* promoter (Fig. 4 E). Notably, high glucose induced a significantly higher level of FOXO1 binding to the *SERPINB2* promoter compared with low glucose (P < 0.05; Fig. 4 E). Consistent with ChIP results, the increase in *SERPINB2* promoter activity in keratinocytes stimulated by high glucose did not occur when *Foxo1* was deleted, also demonstrating FOXO1 dependence (P < 0.05; Fig. 4 F).

Transwell assays were then used to examine the functional impact of SERPINB2 on migration of primary murine keratinocytes from control (K14.Cre⁻.*Foxo1*^L/L) mice. Knockdown of SERPINB2 with siRNA increased migration of keratinocytes from control mice by 2.8-fold in high glucose (P < 0.05; Fig. 4 G), demonstrating that SERPINB2 expression in high glucose limited migration. The result indicates that the negative effect of high glucose on keratinocyte migration is caused in part by high levels of SERPINB2 mediated by FOXO1 in high glucose.

CCL20 was examined for the aforementioned reasons. CCL20 mRNA levels in vitro increased 9.3-fold in human keratinocytes in high glucose media (P < 0.05) and knockdown of FOXO1 blocked this increase (P < 0.05; Fig. 5 A). At the protein level, high glucose induced an almost twofold increase in CCL20 expression in murine keratinocytes (P < 0.05), which was blocked by *Foxo1* deletion (P < 0.05; Fig. 5, B and C). The impact of FOXO1 on CCL20 expression in vivo was then examined in wounds of experimental and control mice. CCL20 levels were increased approximately twofold in diabetic wounds compared with normoglycemic wounds in K14.Cre⁻.*Foxo1*^L/L control mice on both day 4 and 7 after wounding (P < 0.05; Fig. 5 D and Fig. S4 C). Keratinocyte-specific deletion of *Foxo1* blocked the diabetes-induced increase in CCL20 expression in vivo (Fig. 5 D and Fig. S4 C). Thus, hyperglycemia in vivo and high glucose in vitro induced CCL20 expression in a FOXO1-dependent manner. Whether FOXO1 regulates CCL20 transcription was further explored. ChIP results showed that high glucose stimulates FOXO1 binding to the *CCL20* promoter (Fig. 5 E). A reporter assay demonstrated that high glucose induced a significant increase in *CCL20* promoter activity in keratinocytes, which was largely blocked by *Foxo1* ablation (P < 0.05; Fig. 5 F). The results collectively indicate that high glucose regulates CCL20 expression and transcription in a FOXO1-dependent manner. Whether or not FOXO1 regulation of CCL20 represents a mechanism by which FOXO1 affects keratinocyte migration was then tested. CCL20-neutralizing antibody increased keratinocyte migration twofold in high glucose (Fig. 5 G). When combined with the aforementioned results that data suggest that glucose stimulates production of CCL20 in a FOXO1-dependent manner and CCL20 interferes with keratinocyte migration.
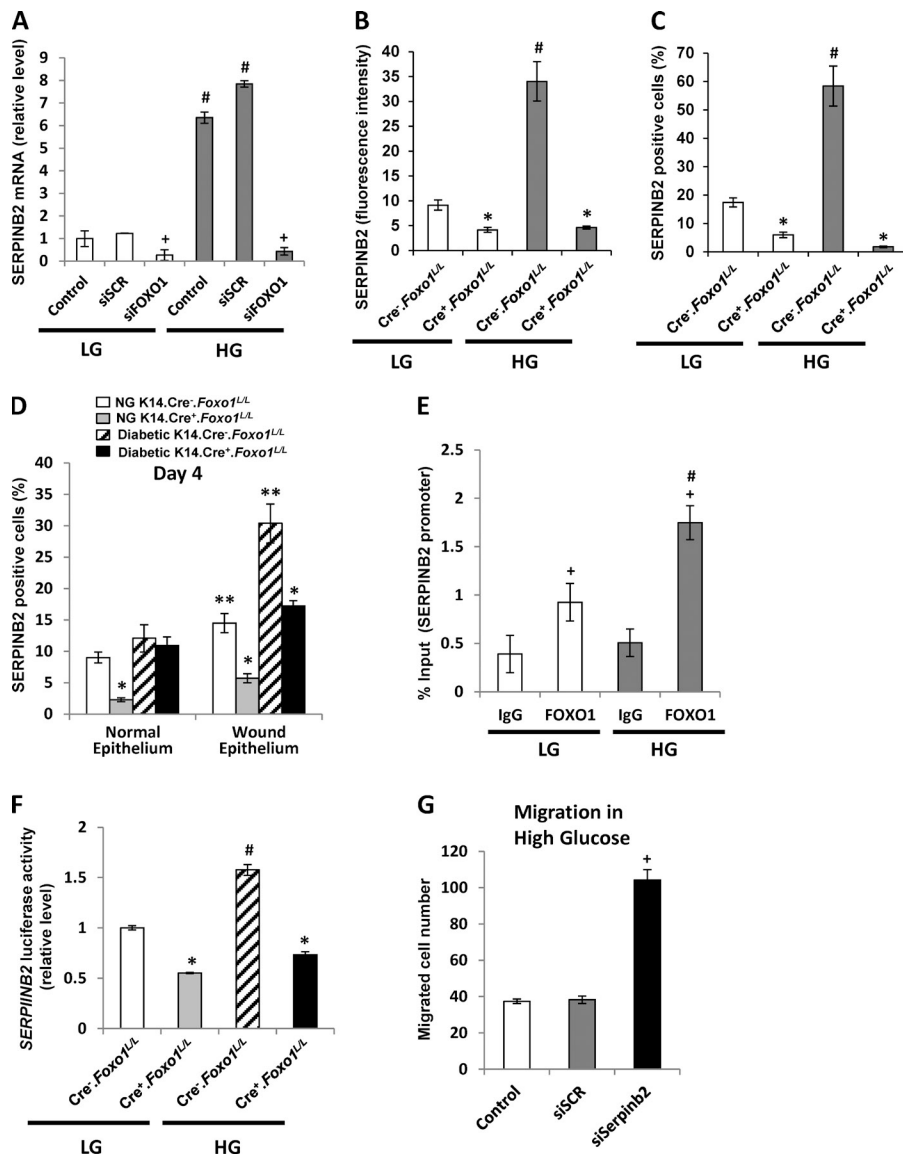
Figure 4. **FOXO1 regulation of SERPINB2 is dependent on glucose levels in vitro and the presence of diabetes in vivo.** NHEK cells (A and E) or primary murine keratinocytes (B, C, F, and G) from K14.Cre$^-$.*Foxo1*$^{L/L}$ or K14.Cre$^+$.*Foxo1*$^{L/L}$ mice were incubated in low or high glucose media. (A) Quantitative RT-PCR analysis of SERPINB2 mRNA levels. (B and C) SERPINB2 immunofluorescence analyses for murine keratinocytes to measure SERPINB2 fluorescence intensity (B) and the number of immunopositive cells (C). (D) SERPINB2 immunofluorescence analyses for day 4 wounds. (E) ChIP assays for the binding of FOXO1 to the *SERPINB2* promoter. (F) *SERPINB2* luciferase reporter gene analyses. (G) Migration was measured by transwell assay for K14.Cre$^-$.*Foxo1*$^{L/L}$ keratinocytes after transfection with scrambled or Serpinb2 siRNA. Each in vivo value is the mean ± SEM for n = 5–8 mice per group. In vitro values represent the mean ± SEM of three independent experiments. $^+$, P < 0.05 versus matched scrambled siRNA or IgG control; $^\#$, P < 0.05 versus matched low glucose group; *, P < 0.05 versus Cre$^-$ group; **, P < 0.05 versus normal epithelium.

Insulin regulates FOXO1 nuclear localization and reverses high glucose-induced expression of FOXO1 and downstream targets SERPINB2 and CCL20

Diabetes involves several factors including low levels of insulin or insulin resistance. The effect of insulin on FOXO1 nuclear localization in keratinocytes in vitro was examined. FOXO1 nuclear localization increased 2.3-fold under stimulation of high glucose when insulin was absent (P < 0.05; Fig. 6 A), whereas mannitol had no effect compared with low glucose (P > 0.05; Fig. S5 A). High glucose-induced FOXO1 nuclear localization was significantly reduced by insulin in a dose-dependent relationship (P < 0.05; Fig. 6 A). In contrast, FOXO1 nuclear localization was barely detected in keratinocytes from K14.Cre$^+$.*Foxo1*$^{L/L}$ mice under all conditions (P > 0.05; Fig. 6 A). These results indicate that the maximum induction of FOXO1 nuclear localization under high glucose conditions is dependent on low levels of insulin signaling.

The effect of insulin on FOXO1 targets SERPINB2 and CCL20 was further investigated. High glucose stimulated the expression of SERPINB2 in keratinocytes from K14.Cre$^-$.*FOXO1*$^{L/L}$ control mice but not by mannitol osmotic control or in keratinocytes from *Foxo1*-deleted mice (Fig. 6 B and Fig. S5 B). Increased SERPINB2 expression stimulated by high glucose was significantly reduced by insulin (P < 0.05; Fig. 6 B). Similarly, high glucose but not mannitol osmotic control stimulated the expression of CCL20 in K14.Cre$^-$.*Foxo1*$^{L/L}$ control keratinocytes but not in *Foxo1*-deleted keratinocytes (P < 0.05; Fig. 6 C and Fig. S5 C). High glucose-induced CCL20 expression was significantly reduced by insulin (P < 0.05; Fig. 6 C). Therefore, insulin regulates the expression of SERPINB2 and CCL20 in a way that coincides with its regulation on FOXO1. The capacity of insulin to rescue the negative effects of high glucose on keratinocyte migration was examined. High glucose inhibited keratinocyte migration by 60% (P < 0.05; Fig. 6 D). Treatment with insulin increased migration in a dose-dependent manner (P < 0.05;

Figure 5. **FOXO1 regulation of CCL20 is dependent on glucose levels in vitro and the presence of diabetes in vivo.** NHEK cells (A and E) or primary murine keratinocytes (B, C, F, and G) from K14.Cre⁻.Foxo1^L/L or K14.Cre⁺.Foxo1^L/L mice were incubated in low or high glucose media. (A) Quantitative RT-PCR analysis of CCL20 mRNA levels. (B and C) CCL20 immunofluorescence analyses for murine keratinocytes to measure CCL20 fluorescence intensity (B) and the number of immunopositive cells (C). (D) CCL20 immunofluorescence analyses for day 4 wounds. (E) ChIP assays for the binding of FOXO1 to the *CCL20* promoter. (F) *CCL20* luciferase reporter gene analyses. (G) Migration was measured by transwell assay for K14.Cre⁻.Foxo1^L/L keratinocytes with or without addition of CCL20-blocking antibody or control IgG. Each in vivo value is the mean ± SEM for n = 5–8 mice per group. In vitro data represent the mean ± SEM of three independent experiments. ⁺, P < 0.05 versus matched scrambled siRNA or IgG control; #, P < 0.05 versus matched low glucose group; *, P < 0.05 versus Cre⁻ group; **, P < 0.05 versus normal epithelium.
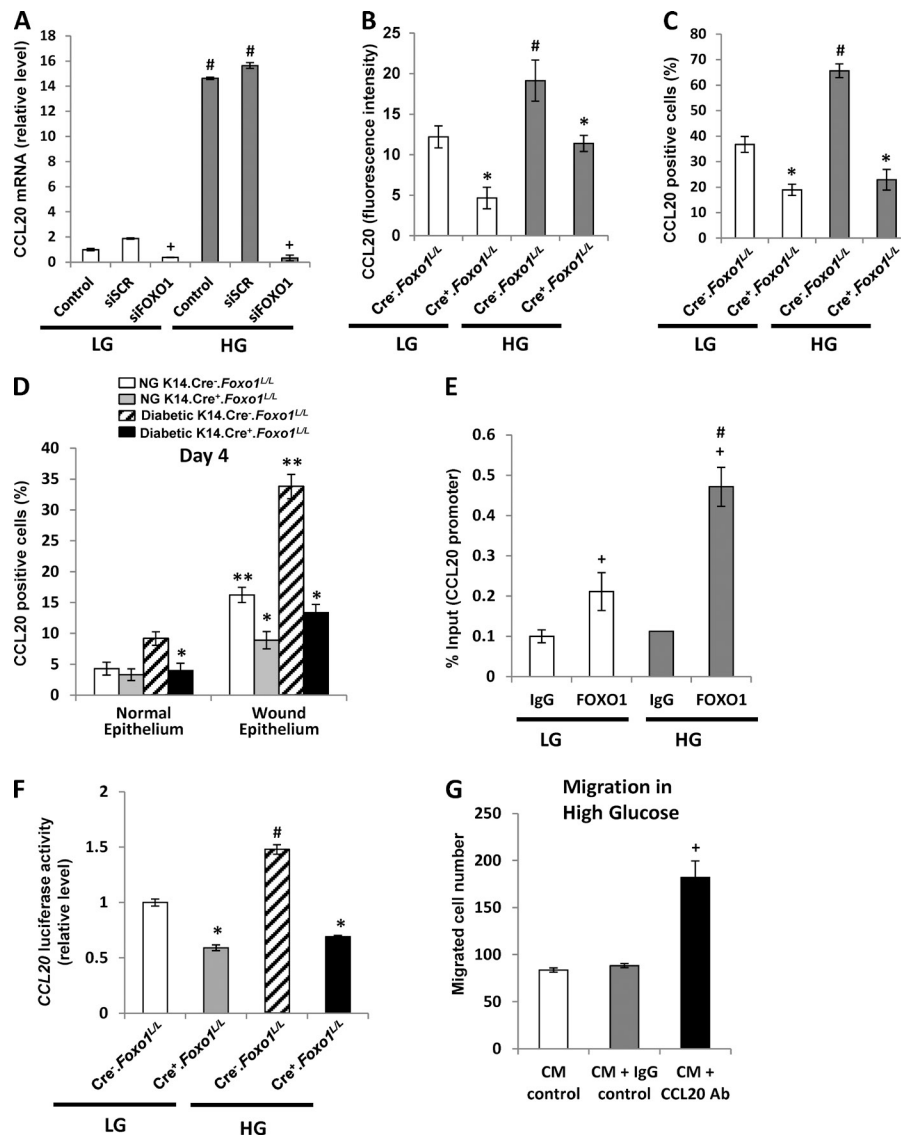

Fig. 6 D). The capacity of insulin to rescue keratinocyte migration in high glucose was blocked by inhibition of AKT (P < 0.05; Fig. 6 D). Akt mediates the inhibitory effect of insulin on FOXO1 (Tsuchiya et al., 2012).

AGE regulates FOXO1 and interferes with keratinocyte migration through FOXO1.

AGEs are elevated in diabetic and aging skin (Bos et al., 2011; Gkogkolou and Böhm, 2012). The effect of an AGE, carboxymethyllysine (CML)-modified BSA (CML-BSA), was tested on FOXO1 and regulation of its target genes, TGFβ1, SERPINB2, and CCL20. AGE stimulated a time-dependent increase in FOXO1 nuclear localization (P < 0.05; Fig. 7 A). In contrast, incubation with AGE reduced TGFβ1 expression at the protein level almost in half in a time-dependent manner (P < 0.05; Fig. 7 A). ChIP experiments determined that the interaction of FOXO1 with *TGFβ1* promoter was largely blocked by AGE treatment (P < 0.05; Fig. 7 C). Consistently with the inhibitory effect of AGE on FOXO1 binding to the *TGFβ1*

promoter, AGE also blocked the capacity of FOXO1 overexpression to stimulate *TGFβ1* promoter activity (Fig. 7 D).

In contrast to the effect on TGFβ1, CML-BSA induced a threefold increase in SERPINB2 and CCL20 protein levels (P < 0.05; Fig. 7, E and F). The capacity of the AGE to induce SERPINB2 and CCL20 was blocked by *FOXO1* deletion (P > 0.05). CML-BSA stimulated FOXO1 binding to both *SERPINB2* and *CCL20* promoters compared with control BSA (P < 0.05; Fig. 7, G and H). Cotransfection of a *FOXO1* expression vector and *SERPINB2* or *CCL20* reporter demonstrated that AGE further enhanced *SERPINB2* and *CCL20* transcriptional activity 65–100% (P < 0.05; Fig. 7, I and J).

The effect of AGE on keratinocyte migration was then investigated. Similar to the effect of high glucose, CML-BSA reduced keratinocyte migration by 65% in wild-type keratinocytes (K14.Cre⁻.Foxo1^L/L; P < 0.05; Fig. 7 K). *Foxo1* ablation reversed the inhibitory effect of AGE on keratinocyte migration (P < 0.05; Fig. 7 K). The role of insulin signaling in keratinocyte migration was then explored. The negative impact of AGE
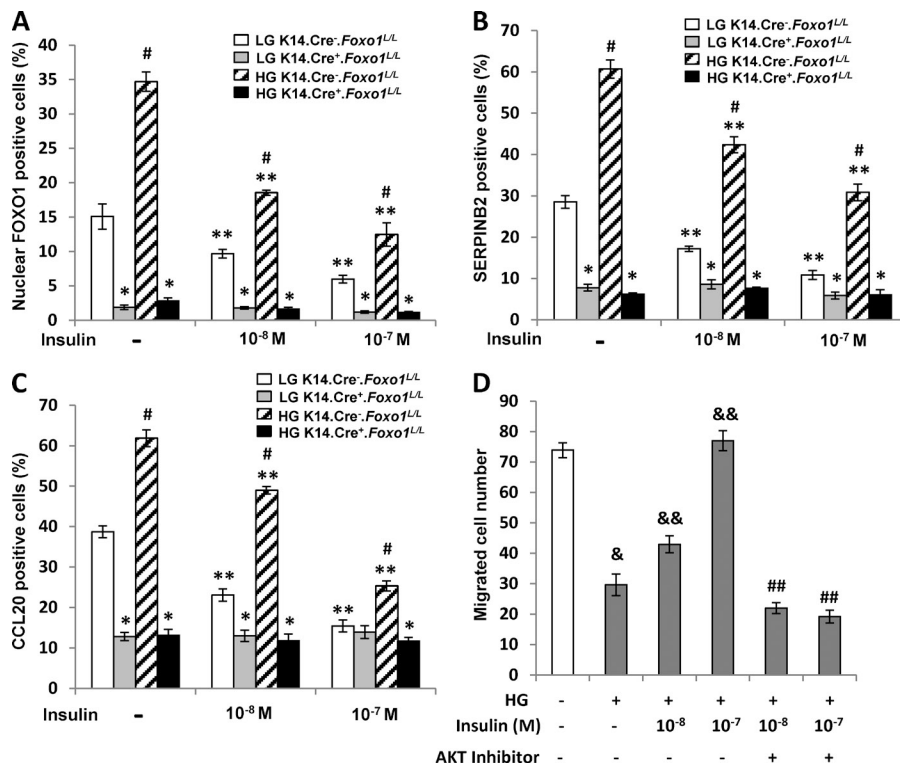
Figure 6. **Insulin regulates FOXO1 nuclear localization and reverses high glucose-induced expression of FOXO1 and downstream targets SERPINB2 and CCL20.** Primary murine keratinocytes isolated from K14.Cre⁻.Foxo1^{L/L} or K14.Cre⁺.Foxo1^{L/l} mice were treated with the indicated doses of insulin for 24 h in low and high glucose media and immunofluorescence analyses were performed to assess FOXO1 nuclear localization (A) and SERPINB2 (B) and CCL20 (C) expression in low and high glucose media. (D) Keratinocyte migration was measured by transwell migration assay in K14. Cre⁻.Foxo1^{L/L} keratinocytes with the addition of insulin with or without AKT inhibitor as indicated. Data show mean ± SEM of three independent experiments. *, $P < 0.05$ versus Cre⁻ group; #, $P < 0.05$ versus low glucose group; **, $P < 0.05$ versus without insulin treatment group; &, $P < 0.05$ versus vehicle control group; &&, $P < 0.05$ versus high glucose alone treatment group; ##, $P < 0.05$ versus high glucose plus insulin treatment group.

on keratinocyte migration was reduced by insulin ($P < 0.05$; Fig. 7 L). Furthermore, the rescue by insulin was blocked by an AKT inhibitor ($P < 0.05$; Fig. 7 L).

TNF regulates FOXO1 and interferes with keratinocyte migration through FOXO1

The effect of TNFα on FOXO1 target genes and FOXO1-mediated keratinocyte migration was examined. FOXO1 nuclear localization was increased approximately threefold by TNF ($P < 0.05$; Fig. 8 A). FOXO1 deletion reduced TGFβ1 protein levels at baseline, which were reduced further by TNF ($P < 0.05$; Fig. 8 B). TNF inhibited the interaction of FOXO1 with *TGFβ1* promoter ($P < 0.05$; Fig. 8 C). The capacity of FOXO1 overexpression to stimulate *TGFβ1* promoter activity was largely blocked by TNF ($P < 0.05$; Fig. 8 D). Thus, TNF negatively regulates TGFβ1 transcriptional activity via FOXO1. However, there are also FOXO1-independent mechanisms because TNF reduced TGFβ1 protein levels further when FOXO1 was knocked down (Fig. 8 B).

Incubation of keratinocytes with TNF increased SERPINB2 and CCL20 protein levels by more than twofold ($P < 0.05$; Fig. 8, E and F). The increase stimulated by TNF was blocked when *Foxo1* was deleted ($P < 0.05$; Fig. 8, E and F). FOXO1 binding to the *SERPINB2* and *CCL20* promoters was significantly increased by TNF ($P < 0.05$; Fig. 8, G and H). The capacity of FOXO1 overexpression to induce *SERPINB2* and *CCL20* promoter activities was enhanced by TNF ($P < 0.05$; Fig. 8, I and J).

The effect of TNF on keratinocyte migration was then explored. TNF reduced keratinocyte migration by 56% ($P < 0.05$), which was FOXO1 dependent ($P < 0.05$; Fig. 8 K). The

negative effect of TNF on keratinocyte migration was partially rescued by incubation with insulin ($P < 0.05$; Fig. 8 L), which was blocked by inhibition of Akt ($P < 0.05$; Fig. 8 L).

Discussion

Results presented here demonstrate that one of the primary differences between normal and diabetic reepithelialization is the role of FOXO1 in the wound healing behavior of keratinocytes. In normal mice, FOXO1 has a positive impact on healing whereas in diabetic mice FOXO1 has the opposite effect and impedes reepithelialization. In normal conditions, deletion of *Foxo1* in keratinocytes reduced wound closure examined grossly or histologically. In contrast, *Foxo1* deletion in diabetic mice enhanced gross wound closure and histological reepithelialization. The effect is caused by the specific role of FOXO1 in keratinocytes because the in vivo model used keratinocyte-specific deletion of *Foxo1* mediated by keratin-14–driven Cre recombinase. Similarly, in standard glucose media, *Foxo1* deletion impaired reepithelialization in vitro, whereas *Foxo1* overexpression enhanced it. *Foxo1* deletion or overexpression in keratinocytes had the opposite effect in high glucose.

The primary difference in FOXO1's effect on reepithelialization of normal and diabetic wounds in vivo and in scratch wounds in vitro can be attributed to its effect on keratinocyte migration. Reduced keratinocyte migration is an important factor in impaired reepithelialization of chronic and diabetic healing (Stojadinovic et al., 2005; Lan et al., 2008; Usui et al., 2008; Jacobsen et al., 2010). We identified two distinct mechanisms through which FOXO1 affects keratinocyte migration, both of which are affected by diabetes in vivo and by high levels of glucose, an AGE, or TNF in vitro. Under normal conditions,
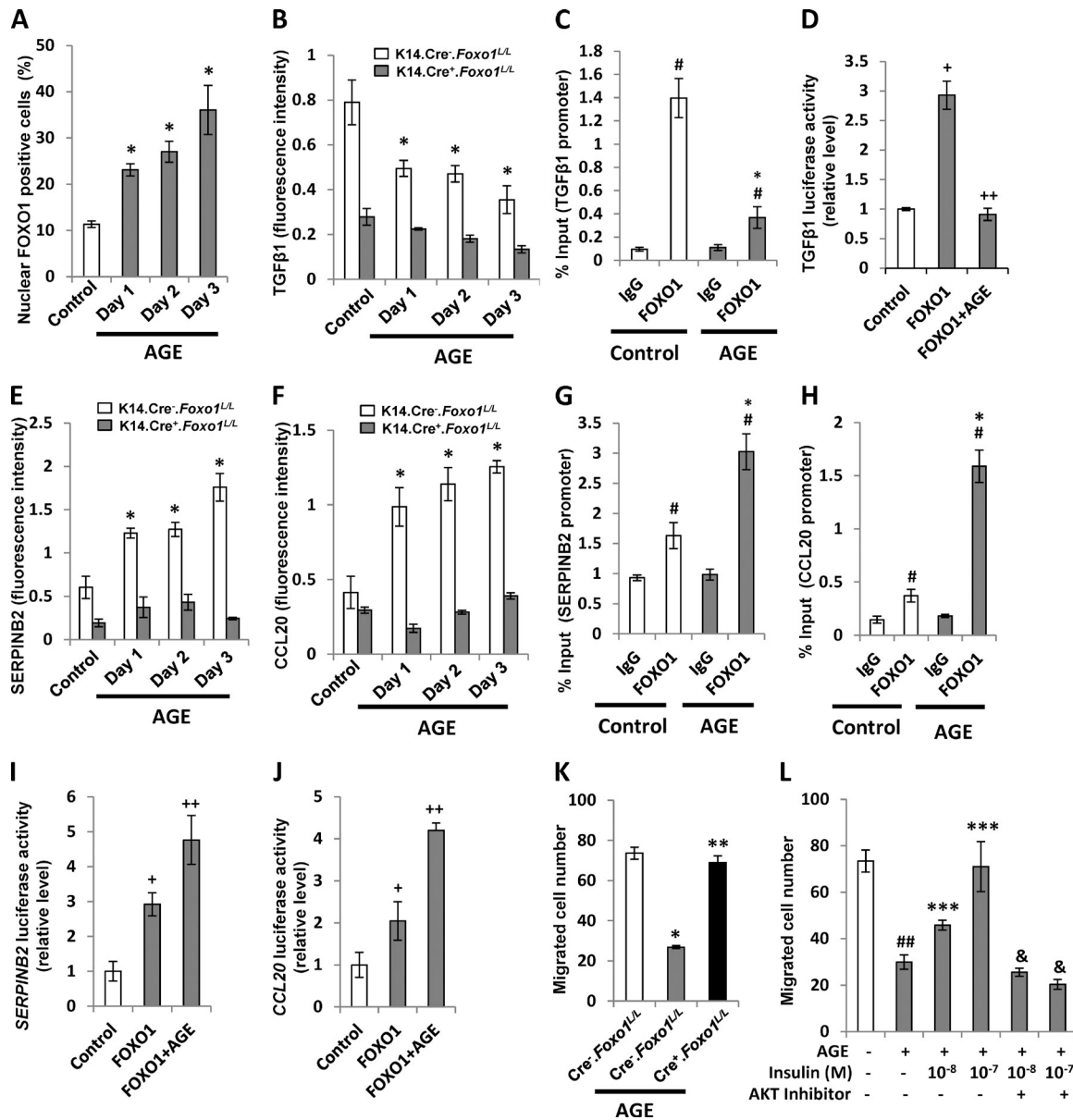
Figure 7. **An AGE stimulates FOXO1 nuclear localization, modulates FOXO1 downstream targets, and reduces keratinocyte migration in a FOXO1-dependent manner.** NHEK cells (A, C, D, and G–J) or primary murine keratinocytes (B, E, F, K, and L) from K14.Cre⁻.Foxo1^{L/L} and K14.Cre⁺.Foxo1^{L/L} mice were incubated with CML-BSA (an AGE) or control unmodified BSA for the indicated time points (A, B, E, and F) or for 3 d (C, D, and G–L). (A) FOXO1 nuclear localization was determined by FOXO1 immunofluorescence and DAPI nuclear staining. (B) TGFβ1 immunofluorescence analyses for murine keratinocytes. (C) ChIP assay to assess FOXO1 binding to the *TGFβ1* promoter. (D) *TGFβ1* luciferase reporter gene analyses after cotransfection with control or FOXO1 plasmid. SERPINB2 (E) and CCL20 (F) immunofluorescence analyses for primary murine keratinocytes. (G and H) ChIP assays for the binding of FOXO1 to the SERPINB2 (G) or CCL20 (H) promoters. *SERPINB2* (I) and *CCL20* (J) luciferase reporter gene analyses after cotransfection with control or FOXO1 plasmid. (K) Murine keratinocyte migration was assessed by transwell migration assay. (L) Keratinocyte migration was measured by transwell migration assay in K14.Cre⁻.Foxo1^{L/L} keratinocytes with the addition of insulin with or without AKT inhibitor as indicated. *, P < 0.05 versus control group; #, P < 0.05 versus IgG control group; +, P < 0.05 versus pcDNA3.1 control group; ++, P < 0.05 versus control group; **, P < 0.05 versus Cre⁻ group; ##, P < 0.05 versus vehicle group; ***, P < 0.05 versus AGE alone treatment group; &, P < 0.05 versus AGE plus insulin treatment group.

FOXO1 binds to the *TGFβ1* promoter and up-regulates TGFβ1 expression. This is significant because TGFβ1 is a potent inducer of keratinocyte migration (Gailit et al., 1994; Decline and Rousselle, 2001; Tredget et al., 2005) and plays an important role in reepithelialization (Sun et al., 2009; Zhang et al., 2012). In contrast, FOXO1 has significantly reduced binding to the *TGFβ1* promoter or induced *TGFβ1* transcription in keratinocytes incubated in high glucose, an AGE, or TNF despite enhanced FOXO1 nuclear translocation. Thus, factors present in diabetes cause the

loss of one of the driving forces of TGFβ1 expression, FOXO1 binding to its promoter to induce transcription. Consistent with this finding is that *Foxo1* ablation in normal mice had significantly reduced phosphorylation of SMAD2/3 (p-SMAD2/3), an immediately downstream target of TGFβ1 receptor signaling. In contrast, deletion of *Foxo1* in diabetic mice did not affect p-SMAD2/3 levels. Moreover, the loss of TGFβ1 signaling caused by FOXO1 has a significant effect because the negative effect of FOXO1 knockdown on keratinocyte migration
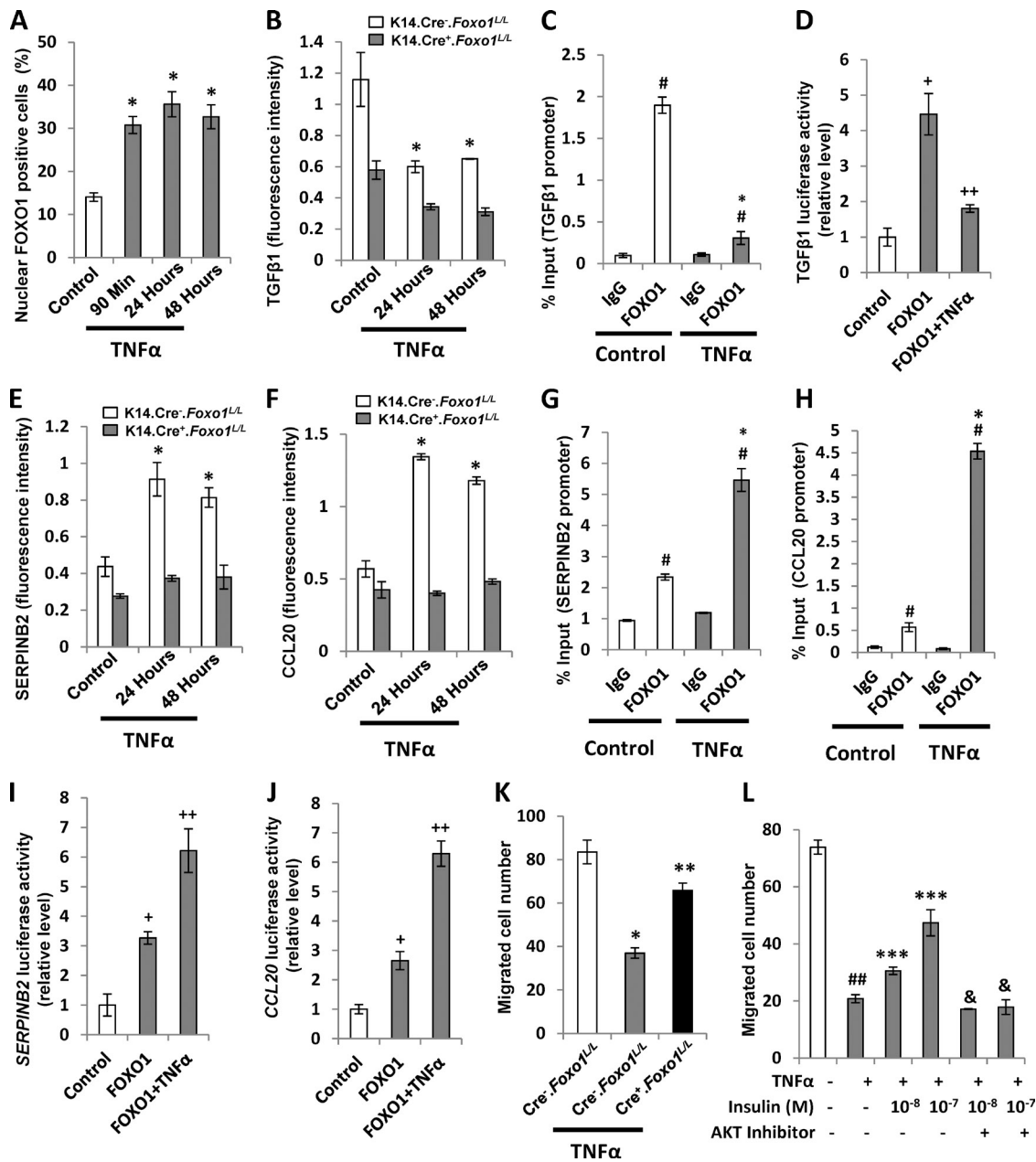
Figure 8. TNF stimulates FOXO1 nuclear localization, modulates FOXO1 downstream targets, and reduces keratinocyte migration in a FOXO1-dependent manner. NHEK cells (A, C, D, and G–J) or primary murine keratinocytes (B, E, F, K, and L) from K14.Cre⁻.Foxo1^L/L and K14.Cre⁺.Foxo1^L/L mice were incubated with TNF for the indicated time points (A, B, E, and F) or for 24 h (C, D, and G–L). (A) FOXO1 nuclear localization was determined by FOXO1 immunofluorescence and DAPI nuclear staining. (B) TGFβ1 immunofluorescence analyses for murine keratinocytes. (C) ChIP assay to assess FOXO1 binding to the *TGFβ1* promoter. (D) *TGFβ1* luciferase reporter gene analyses after cotransfection with control or FOXO1 plasmid. SERPINB2 (E) and CCL20 (F) immunofluorescence analyses for primary murine keratinocytes. (G and H) ChIP assays for the binding of FOXO1 to the SERPINB2 (G) or CCL20 (H) promoters. *SERPINB2* (I) and *CCL20* (J) luciferase reporter gene analyses after cotransfection with control or FOXO1 plasmid. (K) Murine keratinocyte migration was assessed by transwell migration assay. (L) Keratinocyte migration was measured by transwell migration assay in K14.Cre⁻.Foxo1^L/L keratinocytes with the addition of insulin with or without AKT inhibitor as indicated. *, P < 0.05 versus control group; #, P < 0.05 versus IgG control group; +, P < 0.05 versus pcDNA3.1 control group; ++, P < 0.05 versus control group; **, P < 0.05 versus Cre⁻ group; ##, P < 0.05 versus vehicle group; ***, P < 0.05 versus AGE alone treatment group; &, P < 0.05 versus AGE plus insulin treatment group.

is rescued by addition of TGFβ1. The results are also consistent with findings that impaired TGFβ1 signaling is involved in delayed diabetic wound healing and provides a mechanistic basis for this previous observation (Al-Mulla et al., 2011).

Although the capacity of FOXO1 to induce TGFβ1 transcription is reduced in diabetic conditions the opposite occurs with negative regulators of keratinocyte migration. Diabetic

wounds expressed higher levels of SERPINB2 and CCL20 than normoglycemic wounds in vivo, which were restored to normal levels by *Foxo1* deletion. Thus, factors present in diabetes such as high levels of glucose, AGEs, or TNF increase FOXO1 binding to *SERPINB2* and *CCL20* promoters and stimulate increased transcription. Increased expression of SERPINB2 and CCL20 is problematic because it interferes with keratinocyte migration.

This is supported by evidence that reduced migration of keratinocytes in high glucose is rescued by knockdown of SERPINB2 or inhibition of CCL20. That SERPINB2 can inhibit cell migration was previously reported (Praus et al., 1999; Shimizu et al., 2003). High levels of SERPINB2 reduce human prostate cancer cell and fibrosarcoma cell migration (Praus et al., 1999; Shimizu et al., 2003). The inhibitory effect of high CCL20 levels on cell migration has not been previously reported.

Diabetes is characterized by a deficit in insulin signaling caused by a relative absence of insulin or resistance to insulin stimulation. The assays were performed with low insulin or none to reflect this condition. We determined whether insulin affected the impact of elevated levels of glucose, an AGE, or TNF. Insulin reversed the negative effect of each factor on keratinocyte migration. Moreover, this was mediated by Akt because the effect of insulin was blocked by an Akt inhibitor. This finding is significant because Akt blocks FOXO1 activation (Tsuchiya,et al., 2012). Insulin also blocked stimulation of SERPINB2 and CCL20 expression by high glucose, an AGE, and TNF. That reduced insulin is important is shown by diminished FOXO1 nuclear localization when keratinocytes are exposed to insulin. Collectively, these results point out the permissive effect of low insulin in facilitating the negative impact of FOXO1 on the wound healing behavior of keratinocytes. This result may explain previous findings that topical administration of insulin promotes wound healing in diabetic animals mediated by the Akt pathway (Lima et al., 2012) and that topical treatment with insulin improves diabetic wound healing in humans (Paul, 1966; Glasser and Barth, 1982).

In summary, we found that FOXO1 has opposite effects on normal and diabetic wound healing. In normal conditions, FOXO1 promotes wound healing by up-regulating TGFβ1 signaling pathway but fails to do this in diabetic wounds. However, in diabetic wounds or when keratinocytes are exposed to high levels of glucose, AGEs, or TNF, FOXO1 impedes wound healing by inducing overexpression of SERPINB2 and CCL20, which interferes with keratinocyte migration. Thus, the relative change (reduced TGFβ1 and increased SERPINB2/CCL20) caused by the impact of the "diabetic condition" on FOXO1–promoter interactions plays an important role in wound healing. The results suggest that FOXO1 may be a useful therapeutic target to treat diabetic wounds and potentially other complications caused by hyperglycemia and insulin insufficiency/resistance. Accumulating evidence suggests that high levels of activated FOXO1 are linked to several diabetic complications. For example, the early loss of endothelial cells and pericytes that occurs in diabetic retinopathy is significantly reduced by knockdown of FOXO1 with siRNA in vivo (Behl et al., 2009). In diabetic cardiomyopathy, deletion of *Foxo1* in cardiomyocytes rescues high-fat diet–induced declines in cardiac function, which is associated with improved survival (Battiprolu et al., 2012). Moreover, some of the negative effects of diabetes on fracture healing have been linked to FOXO1 (Kayal et al., 2010). FOXO1 is hyperactivated in diabetes because of the stimulatory effects of high glucose and reduced insulin signaling that lead to insufficient inactivation of FOXO1 (Ni et al., 2007). Thus, in diabetic wound healing FOXO1 interferes with keratinocyte migration by enhancing the expression of SERPINB2

and CCL20. In addition, in diabetic conditions, high levels of glucose, AGEs, or TNF, FOXO1 fails to bind to the *TGFβ1* promoter, thus failing to induce a critical wound healing factor. These results point to a previously unrecognized mechanism for delayed diabetic wound healing and the role of FOXO1. In addition, AGEs and TNF are elevated in aging skin (Schnider and Kohn, 1980, 1981; Yarosh et al., 2000; Rittié and Fisher, 2002; Lohwasser et al., 2006) and associated with impaired healing during aging (Goova et al., 2001; Ashcroft et al., 2002; Hardman et al., 2008; Peppa et al., 2009). Thus, the impact of AGEs and TNF on FOXO1-mediated expression of TGFβ1, CCL20, and SERPINB2 may also negatively affect wound healing in the aged.

Materials and methods

Animals and induction of diabetes
Animal experiments were approved by the University of Pennsylvania Institutional Animal Care and Use Committee. Mice with floxed *Foxo1* were provided by R.A. DePinho (MD Anderson Cancer Center, Houston, TX) as previously described (Paik et al., 2007). Mice expressing Cre recombinase under the control of keratin 14 promoter (K14-Cre; strain Tg(KRT14-cre)1Amc/J) were obtained from the Jackson Laboratory. Lineage-specific *Foxo1* deletion was obtained by crossing these mice to generate experimental (K14.Cre$^+$.*Foxo1*$^{L/L}$) and control (K14.Cre$^-$.*Foxo1*$^{L/L}$) mice. Two to five mice were housed per cage under standard conditions with a 14-h light/10-h dark cycle. All the experiments were performed with adult mice 16–20 wk old. Type 1 diabetes was induced by multiple low dose i.p. injections of streptozotocin (40 mg/kg; Sigma-Aldrich) in 10 mM citrate buffer daily for 5 d. Control mice were treated identically with vehicle alone. The blood glucose levels were monitored after completion of multiple low dose streptozotocin or citrate buffer injections (Table S2). Mice were considered to be hyperglycemic when serum glucose levels were >220 mg/dl. Experiments were performed when mice had been hyperglycemic for at least 3 wk.

Skin wounding experiment
Mice were anaesthetized by i.p. administration of ketamine (80 mg/kg) and xylazine (5 mg/kg). The scalp hair was shaved and cleansed, and two excisional wounds were made with a 2-mm sterile biopsy punch in the scalp at the midline as described previously (Siqueira et al., 2010). Wound healing was grossly monitored with calibrated digital photographs at the indicated time points. A ruler was placed next to the specimens and images were captured. NIS-elements software (Nikon) was used to measure wound area at each time point. The mean area of two wounds per animal was measured to establish the wound size for each animal, which was the unit of measurement. Wound size was presented as the percentage of wound area compared with day 0. Animals were euthanized to collect the wound tissue at the indicated time points.

Histology
Excised skin specimens with scalp and attached calvarial bone were fixed in 4% paraformaldehyde for 24 h, decalcified in 10% EDTA solution, and embedded in paraffin. 5-µm paraffin sections were stained with hematoxylin and eosin and histomorphometric analysis was performed with NIS-elements D image analysis software at the center of each lesion.

Immunohistochemistry in histological sections
Paraffin-embedded, formalin-fixed skin sections were processed for immunofluorescence analyses. Antigen retrieval was performed in 10 mM of citric acid, pH 6.0, at 120°C except for CCL20, for which EDTA solution (1 mM; pH 9.0) was used at 120°C. Sections were then incubated with primary antibody to FOXO1 (rabbit; Santa Cruz Biotechnology, Inc.), PCNA (rabbit; Santa Cruz Biotechnology, Inc.), uPAR (rabbit; Santa Cruz Biotechnology, Inc.), TGFβ1 (rabbit; Abcam), phospho-SMAD2/3 (rabbit; Santa Cruz Biotechnology, Inc.), SMAD 2/3 (rabbit; Santa Cruz Biotechnology, Inc.), CCL20 (rabbit; Abcam), and SERPINB2 (goat; Santa Cruz Biotechnology, Inc.) overnight at 4°C as well as the appropriate isotype-matched negative control IgG. Biotinylated secondary antibody (Vector Laboratories) and ABC reagent (Vector Laboratories) were then used. Tyramide signal amplification (PerkinElmer) was also used to enhance the chromogenic signal. Finally, Alexa Fluor 546–conjugated streptavidin (Invitrogen) and DAPI-containing mounting media were used to visualize the staining (Sigma-Aldrich).

Images were taken at 100, 200, and 400 magnification with a fluorescence microscope (ECLIPSE 90i; Nikon) with the same exposure time for experimental and negative control groups. Image analysis was performed using NIS Elements AR image analysis software. The number of immunopositive cells divided by the number of DAPI-positive cells was used to get the percentage of positive cells for each measured antibody. Fluorescence intensity measurements were calculated by subtracting mean fluorescence intensity values of control IgG from values obtained with each antibody.

Cell culture, treatment, and transfection

Primary cultures of NHEK cells were purchased from Lonza and maintained in KGM-2 growth medium supplemented with human keratinocyte growth supplements (Lonza). Primary mouse epidermal keratinocytes were isolated from the neonates (0–2 d old) of experimental (K14.Cre$^+$.Foxo1$^{L/L}$) and control (K14.Cre$^-$.Foxo1$^{L/L}$) mice. In brief, mouse skin was collected and digested with 2.5 U/ml Dispase II (Roche) overnight at 4°C. The dermis was then separated from the epidermis by digesting with 0.1% trypsin and 0.02% EDTA in PBS for 15 min at 37°C. Keratinocytes from the epidermis were cultured in KGM-2 growth medium containing antibiotics. All cell cultures were maintained in a 5% CO$_2$ humidified incubator at 37°C. Keratinocytes were passaged in KGM-2 growth media with supplements including standard insulin (8.6 × 10^{-7} M). For assays, cells were transferred to KGM-2 media with supplements except the amount of insulin was reduced 100-fold unless otherwise stated, i.e., low insulin represents 1% of the amount of insulin in standard keratinocyte growth media. In some experiments no insulin was added.

ON-TARGETplus SMARTpool siRNAs against human FOXO1 and FOXO3 and control siRNA (ON-TARGETplus Non-targeting Control Pool) were obtained from GE Healthcare and transfection was performed using GenMute siRNA Transfection Reagent (SignaGen Laboratories). In most transfection experiments, cells were incubated for 6 h with siRNA and transfection reagent 2 d before assay. Cells were then rinsed and transferred back to the indicated culture media for the remaining incubation period. Plasmid DNA transient transfections were performed using Lipofectin (Invitrogen) according to the manufacturer's instructions. Transfection occurred 2 d before assay.

Immunofluorescence analysis in vitro

Primary keratinocytes isolated from K14.Cre$^-$.Foxo1$^{L/L}$ and K14.Cre$^+$.Foxo1$^{L/L}$ mice were grown on 8-well chamber slides (Thermo Fisher Scientific) and incubated in low glucose (5 mM D-glucose), high glucose (25 mM D-glucose), or osmotic control medium (25 mM D-mannitol) for 5 d. In some experiments, cells were incubated with CML-BSA (200 µg/ml), which was prepared by chemical modification of BSA (Sigma-Aldrich) as previously described (Alikhani et al., 2010), and compared with control cells incubated with unmodified BSA in low insulin. In brief, 50 mg BSA was dissolved in 25 ml HCl (1 mM) freshly made in sterile water and incubated at 37°C with occasional mixing. Sterile PBS, pH 7.8 (25 ml), was added, followed by sodium cyanoborohydride (1.42 g) and sodium glyoxyliate acid (0.715 g). Control BSA was prepared at the same time except that no glyoxyliate acid was added. In some cases, cells were incubated with 10 ng/ml TNF (PreproTech) in low insulin. In experiments measuring the response to insulin, cells were incubated with defined amounts of insulin (Santa Cruz Biotechnology, Inc.) for 24 h before assay and compared with incubation in the same media without insulin. For immunofluorescence, keratinocytes were fixed in 3.7% formaldehyde for 10 min, permeabilized in 0.5% Triton X-100 for 5 min, blocked in 2% BSA, and stained with primary antibody anti-FOXO1 (Santa Cruz Biotechnology, Inc.), TGFβ1 (Abcam), SERPINB2 (Santa Cruz Biotechnology, Inc.), or CCL20 (Abcam). Primary antibody was localized with biotinylated secondary antibody and Alexa Fluor 546–conjugated streptavidin and mounted with DAPI-containing mounting media. Images were captured at a magnification of 200 by a fluorescence microscope with the same exposure time for experimental and negative control groups. Image analysis was performed using NIS Elements AR image analysis software. The percentage of immunopositive cells and mean fluorescence intensity was measured.

In vitro scratch wound assay

NHEK cells were treated with low (5 mM D-glucose) or high (25 mM D-glucose) glucose for 5 d and transfected with FOXO1 or scrambled siRNA. Confluent cells were "scratched" using a 200-µl pipette tip and rinsed with PBS to remove scratched cells as described previously (Liang et al., 2007). Images were captured as indicated to assess the number of keratinocytes that had migrated into the wounded area using NIS-elements D image analysis software.

Keratinocytes transwell migration assay

NHEK cells were incubated in indicated doses of D-glucose (5, 12, 17, and 25 mM) or osmotic control (25 mM D-mannitol) medium for 5 d and transfected with FOXO1 or scrambled siRNA. In some cases, cells were treated with 2 ng/ml TGFβ1 for 24 h after transfection. Migration was then assessed in a transwell assay with a polycarbonate membrane filter (6.5-mm diameter and 8-µm pore size; Corning). In brief, 10^5 cells were placed in the upper chamber of a transwell plate. After 6 h, cells remaining in the upper surface of the membrane were removed with cotton swabs and migrated cells on the lower surface of the membrane were stained with DAPI and counted by fluorescence microscopy. Assays were performed as triplicates.

In some cases, conditioned medium in high glucose conditions was first collected from primary keratinocytes isolated from K14.Cre$^-$.Foxo1$^{L/L}$ mice. The cells were preincubated with 0.4 µg/ml CCL20 blocking antibody (R&D Systems) or matched control IgG and incubated in conditioned medium plus antibody to CCL20 or matched control IgG, which were added to the upper chamber of a transwell plate. In some cases, murine keratinocytes were first transfected with 5 nM Serpinb2 siRNA (Santa Cruz Biotechnology, Inc.), and then the cells were incubated in conditioned medium and added to the upper chamber to measure the effect on keratinocyte migration.

In some experiments, murine keratinocytes isolated from K14.Cre$^-$.Foxo1$^{L/L}$ and K14.Cre$^+$.Foxo1$^{L/L}$ mice were first incubated with high glucose (25 mM D-glucose) for 5 d, CML-BSA (200 µg/ml) for 3 d, or TNF (10 ng/ml) for 1 d before migration assay. In other experiments, keratinocytes were also incubated in high glucose, CML-BSA, or TNF with the addition of insulin (10^{-8} or 10^{-7} M) with or without 5 nM AKT inhibitor triciribine (Abcam) for the final 24 h. After incubation, keratinocyte migration was measured in a transwell migration assay.

DNA binding capacity of FKHR (FOXO1)

The effect of high glucose on FOXO1 binding to DNA was measured by ELISA using TransAM FKHR (FOXO1) Transcription Factor ELISA kit (Active Motif). In brief, nuclear extract of NHEK cells was prepared and DNA binding of FOXO1 was performed following the manufacturer's instructions.

BrdU incorporation assay

DNA synthesis was measured by ELISA using a BrdU Cell Proliferation Assay kit (Cell Signaling Technology). NHEK cells and primary murine keratinocytes isolated from K14.Cre$^-$.Foxo1$^{L/L}$ and K14.Cre$^+$.Foxo1$^{L/L}$ mice were treated in low (5 mM D-glucose) or high (25 mM D-glucose) glucose conditions for 5 d, during which NHEK cells were transfected with FOXO1 or scrambled siRNA. Then, 2 × 10^4 cells were seeded in 96-well plates and incubated with 10 µM BrdU for 6 h. ELISA for BrdU-incorporated keratinocytes was then performed according to the manufacturer's instruction. Experiments were performed three times with similar results.

Western blotting

Primary keratinocytes isolated from K14.Cre$^-$.Foxo1$^{L/L}$ mice were incubated in low (5 mM D-glucose) or high (25 mM D-glucose) glucose medium without insulin for 5 d, and then were lysed with lysis buffer (Thermo Fisher Scientific). The NE-PER Nuclear and Cytoplasmic Extraction Reagent kit (Thermo Fisher Scientific) was used to separately isolate cytoplasmic and nuclear protein fractions. Proteins (50 µg of cell lysate) were resolved by 4–20% SDS-PAGE (Bio-Rad Laboratories) and transferred onto PVDF membrane (Thermo Fisher Scientific). The membranes were incubated with primary antibodies against FOXO1 (Santa Cruz Biotechnology, Inc.), laminine A (Sigma-Aldrich), and actin (Sigma-Aldrich) after blocking with 5% BSA. The samples were then incubated with horseradish peroxidase–labeled anti–mouse IgG, and immunoreactive bands were detected with ECL Western blotting reagents (Thermo Fisher Scientific).

ChIP

ChIP assays were performed using ChIP-IT kit (Active Motif) following the manufacturer's instructions. NHEK cells were incubated in high glucose for 5 d, CML-BSA (200 µg/ml) or unmodified BSA (200 µg/ml) for 24 h, or TNF (10 ng/ml) for 1 h in culture media without insulin before lysing cells. To precipitate FOXO1, anti-FOXO1 antibody (Santa Cruz Biotechnology, Inc.) was used. Quantitative real-time PCR for TGFβ1, SERPINB2, and CCL20 promoters were performed, respectively, using immunoprecipitated chromatin with probes (Roche) and oligonucleotide primers (Integrated DNA Technologies). The following primers were used: TGFβ1 (forward, 5'-CCAT-GTTGACAGACCCTCCT-3'; and reverse, 5'-TTAATCCGGGGGATGAGAC-3');

SERPINB2 (forward, 5′-GAAGCAGGAAAGCAGAAAGAAG-3′; and reverse, 5′-ACTGCCACACAGGAAGATATAC-3′); and *CCL20* (forward, 5′-TCTGATATAGGCATCACCAACTC-3′; and reverse, 5′-GAACTCTCCA-CTAGACCCAAATAG-3′).

Luciferase reporter assay

Transient transfection with luciferase reporter constructs was performed using Lipofectin (Invitrogen) in 24-well plates. In brief, NHEK cells were incubated in culture media without insulin for 5 d with 5 or 25 mM D-glucose or with CML-BSA (200 µg/ml) for 3 d or TNF (10 ng/ml) for 24 h before assay. Cells were cotransfected with *TGFβ1* luciferase reporter (provided by D. Sinnett, University of Montreal, Montreal, Quebec, Canada), *SERPINB2* luciferase reporter (provided by T.M. Antalis, University of Maryland School of Medicine, Baltimore, MD), or *CCL20* luciferase reporter (provided by J.-M. Wang, National Cheng Kung University, Tainan, Taiwan) together with pRL-TK luciferase control vector, FOXO1-AAA plasmid that is constitutively transported to the nucleus, or pcDNA3.1 control plasmid. 2 d after transfection, cells were lysed, and *Firefly* and *Renilla* luciferase activities were measured using Dual Luciferase Reporter Assay kit (Promega) according to the manufacturer's instructions. *Firefly* luciferase activities were divided by *Renilla* activities to normalize for transfection efficiency. Experiments were performed three times with similar results. In some experiments, primary murine keratinocytes from K14.Cre⁻.Foxo1$^{L/L}$ and K14.Cre⁺.Foxo1$^{L/L}$ mice in low (5 mM D-glucose) or high (25 mM D-glucose) glucose medium were cotransfected with *SERPINB2* or *CCL20* luciferase reporter and pRL-TK luciferase control vector. 2 d after transfection, cells were lysed and tested with the Dual Luciferase Reporter Assay.

Microarray analysis and real-time PCR

NHEK cells were incubated in low (5 mM D-glucose) or high (25 mM D-glucose) glucose medium for 5 d and transfected with FOXO1 or scrambled siRNA. Total RNA was then isolated using an RNeasy kit (QIAGEN). RNA profiling was performed using a GeneChIP Human Gene 1.0 ST array (Affymetrix). The identification of genes that were up- or down-regulated by high glucose and FOXO1 knockdown was defined as those that were both up-regulated (>1.3-fold) by high glucose and down-regulated (<0.7-fold) by *FOXO1* siRNA with P < 0.05, both when compared with the matched control group. Real-time quantitative RT-PCR of selected genes was performed to validate microarray results using Taqman primers and probes (Roche). All primers were designed using the Universal Probe Library Assay Design Center (Roche). Results were normalized with respect to the value obtained for the housekeeping gene RPL32, a ribosomal protein. Each experiment was performed two to four times with similar results.

Statistics

Statistical analysis between two groups was performed using two-tailed Student's *t* test. In experiments with multiple time points or treatments, differences between the wild-type and experimental groups were determined by analysis of variance with Scheffe's post-hoc test. Results were expressed as the mean ± SEM. P < 0.05 was considered statistically significant.

Online supplemental material

Fig. S1 demonstrates the effect of keratinocyte-specific *Foxo1* deletion on normoglycemic and diabetic wound healing and its effect on FOXO1 expression. Fig. S2 presents the impact of high glucose on in vitro reepithelialization. Fig. S3 demonstrates the effect of keratinocytes-specific deletion of *Foxo1* on uPAR expression in wounded epithelium, a marker of keratinocyte migration, in vivo. It also demonstrates the impact of FOXO1 knockdown on keratinocyte migration and proliferation in vitro. Fig. S4 shows the effect of keratinocyte-specific *Foxo1* deletion on SERPINB2 and CCL20 expression in normoglycemic and diabetic mice. Fig. S5 measures the effect of insulin on FOXO1 nuclear localization and the expression of SERPINB2 and CCL20 in keratinocytes incubated in standard glucose media or media supplemented with mannitol osmotic control. Table S1 presents a list of genes that were up-regulated in high glucose conditions and down-regulated by FOXO1 knockdown. Table S2 shows the blood glucose levels of the mice after multiple low dose streptozotocin or citrate buffer injections. Online supplemental material is available at http://www.jcb.org/cgi/content/full/jcb.201409032/DC1.

References

Al-Mulla, F., S.J. Leibovich, I.M. Francis, and M.S. Bitar. 2011. Impaired TGF-β signaling and a defect in resolution of inflammation contribute to delayed wound healing in a female rat model of type 2 diabetes. *Mol. Biosyst.* 7:3006–3020. http://dx.doi.org/10.1039/c0mb00317d

Alikhani, M., Z. Alikhani, C. Boyd, C.M. MacLellan, M. Raptis, R. Liu, N. Pischon, P.C. Trackman, L. Gerstenfeld, and D.T. Graves. 2007. Advanced glycation end products stimulate osteoblast apoptosis via the MAP kinase and cytosolic apoptotic pathways. *Bone.* 40:345–353. http://dx.doi.org/10.1016/j.bone.2006.09.011

Alikhani, M., S. Roy, and D.T. Graves. 2010. FOXO1 plays an essential role in apoptosis of retinal pericytes. *Mol. Vis.* 16:408–415.

Andriessen, M.P., B.H. van Bergen, K.I. Spruijt, I.H. Go, J. Schalkwijk, and P.C. van de Kerkhof. 1995. Epidermal proliferation is not impaired in chronic venous ulcers. *Acta Derm. Venereol.* 75:459–462.

Ashcroft, G.S., S.J. Mills, and J.J. Ashworth. 2002. Ageing and wound healing. *Biogerontology.* 3:337–345. http://dx.doi.org/10.1023/A:1021399228395

Ashcroft, G.S., M.J. Jeong, J.J. Ashworth, M. Hardman, W. Jin, N. Moutsopoulos, T. Wild, N. McCartney-Francis, D. Sim, G. McGrady, et al. 2012. Tumor necrosis factor-alpha (TNF-α) is a therapeutic target for impaired cutaneous wound healing. *Wound Repair Regen.* 20:38–49. http://dx.doi.org/10.1111/j.1524-475X.2011.00748.x

Barthel, A., D. Schmoll, and T.G. Unterman. 2005. FoxO proteins in insulin action and metabolism. *Trends Endocrinol. Metab.* 16:183–189. http://dx.doi.org/10.1016/j.tem.2005.03.010

Battiprolu, P.K., B. Hojayev, N. Jiang, Z.V. Wang, X. Luo, M. Iglewski, J.M. Shelton, R.D. Gerard, B.A. Rothermel, T.G. Gillette, et al. 2012. Metabolic stress-induced activation of FoxO1 triggers diabetic cardiomyopathy in mice. *J. Clin. Invest.* 122:1109–1118. http://dx.doi.org/10.1172/JCI60329

Behl, Y., P. Krothapalli, T. Desta, S. Roy, and D.T. Graves. 2009. FOXO1 plays an important role in enhanced microvascular cell apoptosis and microvascular cell loss in type 1 and type 2 diabetic rats. *Diabetes.* 58:917–925. http://dx.doi.org/10.2337/db08-0537

Bos, D.C., W.L. de Ranitz-Greven, and H.W. de Valk. 2011. Advanced glycation end products, measured as skin autofluorescence and diabetes complications: a systematic review. *Diabetes Technol. Ther.* 13:773–779. http://dx.doi.org/10.1089/dia.2011.0034

Coulombe, P.A. 2003. Wound epithelialization: accelerating the pace of discovery. *J. Invest. Dermatol.* 121:219–230. http://dx.doi.org/10.1046/j.1523-1747.2003.12387.x

Dasu, M.R., and I. Jialal. 2013. Amelioration in wound healing in diabetic toll-like receptor-4 knockout mice. *J. Diabetes Complications.* 27:417–421. http://dx.doi.org/10.1016/j.jdiacomp.2013.05.002

Decline, F., and P. Rousselle. 2001. Keratinocyte migration requires α2β1 integrin-mediated interaction with the laminin 5 γ2 chain. *J. Cell Sci.* 114:811–823.

Eijkelenboom, A., and B.M. Burgering. 2013. FOXOs: signalling integrators for homeostasis maintenance. *Nat. Rev. Mol. Cell Biol.* 14:83–97. http://dx.doi.org/10.1038/nrm3507

Gailit, J., M.P. Welch, and R.A. Clark. 1994. TGF-β1 stimulates expression of keratinocyte integrins during re-epithelialization of cutaneous wounds. *J. Invest. Dermatol.* 103:221–227. http://dx.doi.org/10.1111/1523-1747.ep12393176

Gary Sibbald, R., and K.Y. Woo. 2008. The biology of chronic foot ulcers in persons with diabetes. *Diabetes Metab. Res. Rev.* **24**(S1, Suppl 1):S25–S30. http://dx.doi.org/10.1002/dmrr.847

Gkogkolou, P., and M. Böhm. 2012. Advanced glycation end products: Key players in skin aging? *Dermatoendocrinol.* 4:259–270. http://dx.doi.org/10.4161/derm.22028

Glasser, J., and A. Barth. 1982. Diabetic wound healing and the case for supplemental treatment with topical insulin. *J. Foot Surg.* 21:117–121.

Goova, M.T., J. Li, T. Kislinger, W. Qu, Y. Lu, L.G. Bucciarelli, S. Nowygrod, B.M. Wolf, X. Caliste, S.F. Yan, et al. 2001. Blockade of receptor for advanced glycation end-products restores effective wound healing in diabetic mice. *Am. J. Pathol.* 159:513–525. http://dx.doi.org/10.1016/S0002-9440(10)61723-3

Goren, I., E. Müller, D. Schiefelbein, U. Christen, J. Pfeilschifter, H. Mühl, and S. Frank. 2007. Systemic anti-TNFα treatment restores diabetes-impaired skin repair in *ob/ob* mice by inactivation of macrophages. *J. Invest. Dermatol.* 127:2259–2267. http://dx.doi.org/10.1038/sj.jid.5700842

Hardman, M.J., E. Emmerson, L. Campbell, and G.S. Ashcroft. 2008. Selective estrogen receptor modulators accelerate cutaneous wound healing in ovariectomized female mice. *Endocrinology.* 149:551–557. http://dx.doi.org/10.1210/en.2007-1042

Huang, H., and D.J. Tindall. 2007. Dynamic FoxO transcription factors. *J. Cell Sci.* 120:2479–2487. http://dx.doi.org/10.1242/jcs.001222

Jacobsen, J.N., B. Steffensen, L. Häkkinen, K.A. Krogfelt, and H.S. Larjava. 2010. Skin wound healing in diabetic β6 integrin-deficient mice. *APMIS.* 118:753–764. http://dx.doi.org/10.1111/j.1600-0463.2010.02654.x

Kayal, R.A., M. Siqueira, J. Alblowi, J. McLean, N. Krothapalli, D. Faibish, T.A. Einhorn, L.C. Gerstenfeld, and D.T. Graves. 2010. TNF-α mediates diabetes-enhanced chondrocyte apoptosis during fracture healing and stimulates chondrocyte apoptosis through FOXO1. *J. Bone Miner. Res.* 25:1604–1615. http://dx.doi.org/10.1002/jbmr.59

Lan, C.C., I.H. Liu, A.H. Fang, C.H. Wen, and C.S. Wu. 2008. Hyperglycaemic conditions decrease cultured keratinocyte mobility: implications for impaired wound healing in patients with diabetes. *Br. J. Dermatol.* 159:1103–1115.

Liang, C.C., A.Y. Park, and J.L. Guan. 2007. In vitro scratch assay: a convenient and inexpensive method for analysis of cell migration in vitro. *Nat. Protoc.* 2:329–333. http://dx.doi.org/10.1038/nprot.2007.30

Lima, M.H., A.M. Caricilli, L.L. de Abreu, E.P. Araújo, F.F. Pelegrinelli, A.C. Thirone, D.M. Tsukumo, A.F. Pessoa, M.F. dos Santos, M.A. de Moraes, et al. 2012. Topical insulin accelerates wound healing in diabetes by enhancing the AKT and ERK pathways: a double-blind placebo-controlled clinical trial. *PLoS ONE.* 7:e36974. http://dx.doi.org/10.1371/journal.pone.0036974

Lohwasser, C., D. Neureiter, B. Weigle, T. Kirchner, and D. Schuppan. 2006. The receptor for advanced glycation end products is highly expressed in the skin and upregulated by advanced glycation end products and tumor necrosis factor-alpha. *J. Invest. Dermatol.* 126:291–299. http://dx.doi.org/10.1038/sj.jid.5700070

Lund, L.R., K.A. Green, A.A. Stoop, M. Ploug, K. Almholt, J. Lilla, B.S. Nielsen, I.J. Christensen, C.S. Craik, Z. Werb, et al. 2006. Plasminogen activation independent of uPA and tPA maintains wound healing in gene-deficient mice. *EMBO J.* 25:2686–2697. http://dx.doi.org/10.1038/sj.emboj.7601173

Moulik, P.K., R. Mtonga, and G.V. Gill. 2003. Amputation and mortality in new-onset diabetic foot ulcers stratified by etiology. *Diabetes Care.* 26:491–494. http://dx.doi.org/10.2337/diacare.26.2.491

Ni, Y.G., N. Wang, D.J. Cao, N. Sachan, D.J. Morris, R.D. Gerard, M. Kuro-O, B.A. Rothermel, and J.A. Hill. 2007. FoxO transcription factors activate Akt and attenuate insulin signaling in heart by inhibiting protein phosphatases. *Proc. Natl. Acad. Sci. USA.* 104:20517–20522. http://dx.doi.org/10.1073/pnas.0610290104

Paik, J.H., R. Kollipara, G. Chu, H. Ji, Y. Xiao, Z. Ding, L. Miao, Z. Tothova, J.W. Horner, D.R. Carrasco, et al. 2007. FoxOs are lineage-restricted redundant tumor suppressors and regulate endothelial cell homeostasis. *Cell.* 128:309–323. http://dx.doi.org/10.1016/j.cell.2006.12.029

Paul, T.N. 1966. Treatment by local application of insulin of an infected wound in a diabetic. *Lancet.* 2:574–576. http://dx.doi.org/10.1016/S0140-6736(66)93041-8

Peppa, M., P. Stavroulakis, and S.A. Raptis. 2009. Advanced glycoxidation products and impaired diabetic wound healing. *Wound Repair Regen.* 17:461–472. http://dx.doi.org/10.1111/j.1524-475X.2009.00518.x

Ponugoti, B., G. Dong, and D.T. Graves. 2012. Role of forkhead transcription factors in diabetes-induced oxidative stress. *Exp. Diabetes Res.* 2012:939751. http://dx.doi.org/10.1155/2012/939751

Ponugoti, B., F. Xu, C. Zhang, C. Tian, S. Pacios, and D.T. Graves. 2013. FOXO1 promotes wound healing through the up-regulation of TGF-β1 and prevention of oxidative stress. *J. Cell Biol.* 203:327–343. http://dx.doi.org/10.1083/jcb.201305074

Praus, M., K. Wauterickx, D. Collen, and R.D. Gerard. 1999. Reduction of tumor cell migration and metastasis by adenoviral gene transfer of plasminogen activator inhibitors. *Gene Ther.* 6:227–236. http://dx.doi.org/10.1038/sj.gt.3300802

Raja, K. Sivamani, M.S. Garcia, and R.R. Isseroff. 2007. Wound re-epithelialization: modulating keratinocyte migration in wound healing. *Front. Biosci.* 12:2849–2868. http://dx.doi.org/10.2741/2277

Reinke, J.M., and H. Sorg. 2012. Wound repair and regeneration. *Eur. Surg. Res.* 49:35–43. http://dx.doi.org/10.1159/000339613

Rittié, L., and G.J. Fisher. 2002. UV-light-induced signal cascades and skin aging. *Ageing Res. Rev.* 1:705–720. http://dx.doi.org/10.1016/S1568-1637(02)00024-7

Schnider, S.L., and R.R. Kohn. 1980. Glucosylation of human collagen in aging and diabetes mellitus. *J. Clin. Invest.* 66:1179–1181. http://dx.doi.org/10.1172/JCI109950

Schnider, S.L., and R.R. Kohn. 1981. Effects of age and diabetes mellitus on the solubility and nonenzymatic glucosylation of human skin collagen. *J. Clin. Invest.* 67:1630–1635. http://dx.doi.org/10.1172/JCI110198

Shimizu, T., K. Sato, T. Suzuki, K. Tachibana, and K. Takeda. 2003. Induction of plasminogen activator inhibitor-2 is associated with suppression of invasive activity in TPA-mediated differentiation of human prostate cancer cells. *Biochem. Biophys. Res. Commun.* 309:267–271. http://dx.doi.org/10.1016/j.bbrc.2003.08.004

Siqueira, M.F., J. Li, L. Chehab, T. Desta, T. Chino, N. Krothapalli, Y. Behl, M. Alikhani, J. Yang, C. Braasch, and D.T. Graves. 2010. Impaired wound healing in mouse models of diabetes is mediated by TNF-α dysregulation and associated with enhanced activation of forkhead box O1 (FOXO1). *Diabetologia.* 53:378–388. http://dx.doi.org/10.1007/s00125-009-1529-y

Stojadinovic, O., H. Brem, C. Vouthounis, B. Lee, J. Fallon, M. Stallcup, A. Merchant, R.D. Galiano, and M. Tomic-Canic. 2005. Molecular pathogenesis of chronic wounds: the role of β-catenin and c-*myc* in the inhibition of epithelialization and wound healing. *Am. J. Pathol.* 167:59–69. http://dx.doi.org/10.1016/S0002-9440(10)62953-7

Sun, T., S. Adra, R. Smallwood, M. Holcombe, and S. MacNeil. 2009. Exploring hypotheses of the actions of TGF-β1 in epidermal wound healing using a 3D computational multiscale model of the human epidermis. *PLoS ONE.* 4:e8515. http://dx.doi.org/10.1371/journal.pone.0008515

Tarcic, G., R. Avraham, G. Pines, I. Amit, T. Shay, Y. Lu, Y. Zwang, M. Katz, N. Ben-Chetrit, J. Jacob-Hirsch, et al. 2012. EGR1 and the ERK-ERF axis drive mammary cell migration in response to EGF. *FASEB J.* 26:1582–1592. http://dx.doi.org/10.1096/fj.11-194654

Tredget, E.B., J. Demare, G. Chandran, E.E. Tredget, L. Yang, and A. Ghahary. 2005. Transforming growth factor-β and its effect on reepithelialization of partial-thickness ear wounds in transgenic mice. *Wound Repair Regen.* 13:61–67. http://dx.doi.org/10.1111/j.1067-1927.2005.130108.x

Tsuchiya, K., J. Tanaka, Y. Shuiqing, C.L. Welch, R.A. DePinho, I. Tabas, A.R. Tall, I.J. Goldberg, and D. Accili. 2012. FoxOs integrate pleiotropic actions of insulin in vascular endothelium to protect mice from atherosclerosis. *Cell Metab.* 15:372–381. http://dx.doi.org/10.1016/j.cmet.2012.01.018

Usui, M.L., J.N. Mansbridge, W.G. Carter, M. Fujita, and J.E. Olerud. 2008. Keratinocyte migration, proliferation, and differentiation in chronic ulcers from patients with diabetes and normal wounds. *J. Histochem. Cytochem.* 56:687–696. http://dx.doi.org/10.1369/jhc.2008.951194

Xu, F., C. Zhang, and D.T. Graves. 2013. Abnormal cell responses and role of TNF-α in impaired diabetic wound healing. *Biomed Res. Int.* 2013:754802. http://dx.doi.org/10.1155/2013/754802

Yamazaki, T., X.O. Yang, Y. Chung, A. Fukunaga, R. Nurieva, B. Pappu, N. Martin-Orozco, H.S. Kang, L. Ma, A.D. Panopoulos, et al. 2008. CCR6 regulates the migration of inflammatory and regulatory T cells. *J. Immunol.* 181:8391–8401. http://dx.doi.org/10.4049/jimmunol.181.12.8391

Yarosh, D., D. Both, J. Kibitel, C. Anderson, C. Elmets, D. Brash, and D. Brown. 2000. Regulation of TNFα production and release in human and mouse keratinocytes and mouse skin after UV-B irradiation. *Photodermatol. Photoimmunol. Photomed.* 16:263–270. http://dx.doi.org/10.1034/j.1600-0781.2000.160606.x

Zhang, C., C.K. Tan, C. McFarlane, M. Sharma, N.S. Tan, and R. Kambadur. 2012. Myostatin-null mice exhibit delayed skin wound healing through the blockade of transforming growth factor-β signaling by decorin. *Am. J. Physiol. Cell Physiol.* 302:C1213–C1225. http://dx.doi.org/10.1152/ajpcell.00179.2011